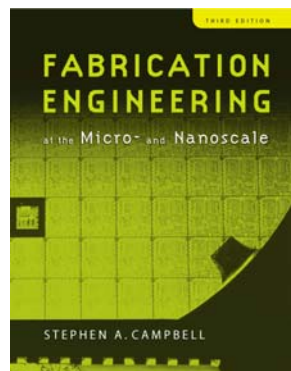


ECE 416/516
IC Technologies
Lecture 13/14:
Physical Vapor Deposition (PVD)

Professor James E. Morris
Spring 2012

Chapter 12

Physical Deposition: Evaporation and Sputtering



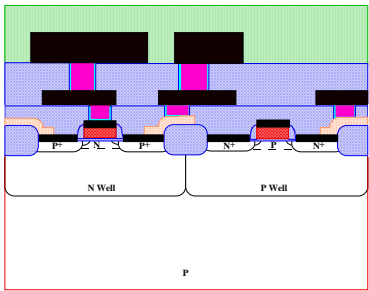
Lecture Topics

- Evaporation Sources
- Evaporation Rate
- Deposited Thicknesses
- Alloy composition & contamination
- Deposition thickness/rate monitors
- Homogeneous nucleation
- Heterogeneous nucleation
 - Capillary theory
 - Spherical cap nuclei
 - Shapes, charge, fields
 - Nucleation rate
 - Atomistic theory
 - Kinetic theory
- Sputtering systems
- Sputtering processes
- Sputtering yield
- Effects of bias, etc.
- Thornton diagram
- Contamination
- Stress

Lecture Objectives

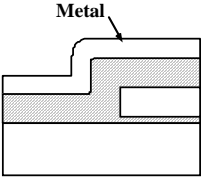
- Can calculate evaporation and deposition rates, thickness, variations, and contamination
- Have knowledge of standard PVD hardware and techniques
- Able to explain nucleation and growth concepts
- Distinguish homogeneous and heterogeneous nucleation
- Can calculate critical nucleus sizes and nucleation rates for capillary, atomistic and kinetic models.
- Be able to explain physics of sputtering, yields, and various system configurations
- Anticipate the effects of bias, contamination and stress

THIN FILM DEPOSITION: Introduction

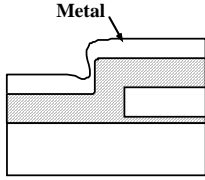


- Many films, made of many different materials, are deposited during a standard CMOS process
- Requirements or desirable traits for deposition:
 1. Desired composition, low contaminants, good electrical and mechanical properties.
 2. Uniform thickness across wafer, and wafer-to-wafer.
 3. Good step coverage (“conformal coverage”).
 4. Good filling of spaces.
 5. Planarized films .

a) Metal

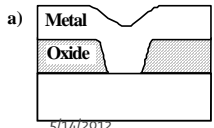


b) Metal

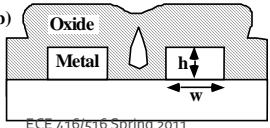


Step Coverage Issues

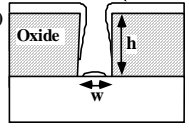
a) Metal
Oxide



b) Oxide
Metal



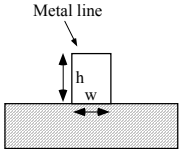
c) Metal
Oxide



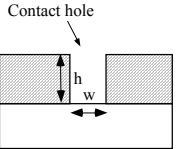
Filling Issues

5/14/2012 ECE 416/516 Spring 2011 5

Metal line



Contact hole



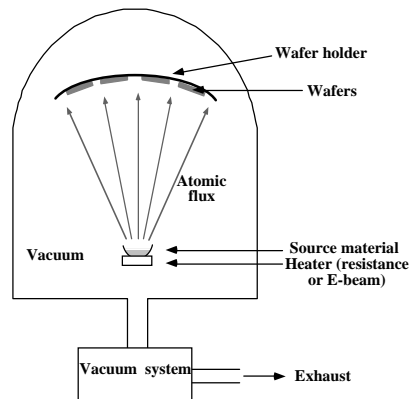
$$\text{Aspect ratio} = AR = \frac{h}{w}$$

Year of Production	1998	2000	2002	2004	2007	2010	2013	2016	2018
Technology Node (half pitch)	250 nm	180 nm	130 nm	90 nm	65 nm	45 nm	32 nm	22 nm	18 nm
MPU Printed Gate Length		100 nm	70 nm	53 nm	35 nm	25 nm	18 nm	13 nm	10 nm
Min Metal 1 Pitch (nm)				214	152	108	76	54	42
Wiring Levels - Logic				10	11	12	12	14	14
Metal 1 Aspect Ratio (Cu)				1.7	1.7	1.8	1.9	2.0	2.0
Contact Aspect Ratio (DRAM)				15	16	>20	>20	>20	>20
STI Trench Aspect Ratio				4.8	5.9	7.9	10.3	14	16.4
Metal Resistivity (μohm-cm)	3.3, 2.2	2.2	2.2	2.2	2.2	2.2	2.2	2.2	2.2
Interlevel Dielectric Constant	3.9	3.7	3.7	<2.7	<2.4	<2.1	<1.9	<1.7	<1.7

- Note the aspect ratios and the need for new materials.
- Note also the number of metal layers requiring more deposition steps.

5/14/2012 ECE 416/516 Spring 2011 6

Physical Vapor Deposition (PVD)



- PVD uses mainly physical processes to produce reactant species in the gas phase and to deposit films.
- In evaporation, source material is heated in high vacuum chamber. ($P < 10^{-5}$ torr)
- Mostly line-of-sight deposition since pressure is low.
- Deposition rate is determined by emitted flux and by geometry of the target and wafer holder.

5/14/2012

ECE 416/516 Spring 2011

7

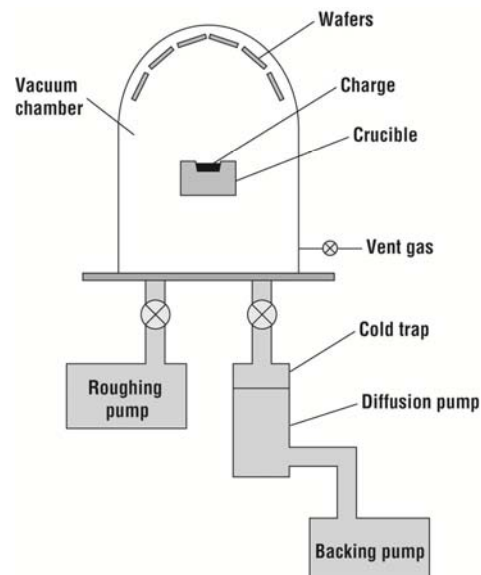


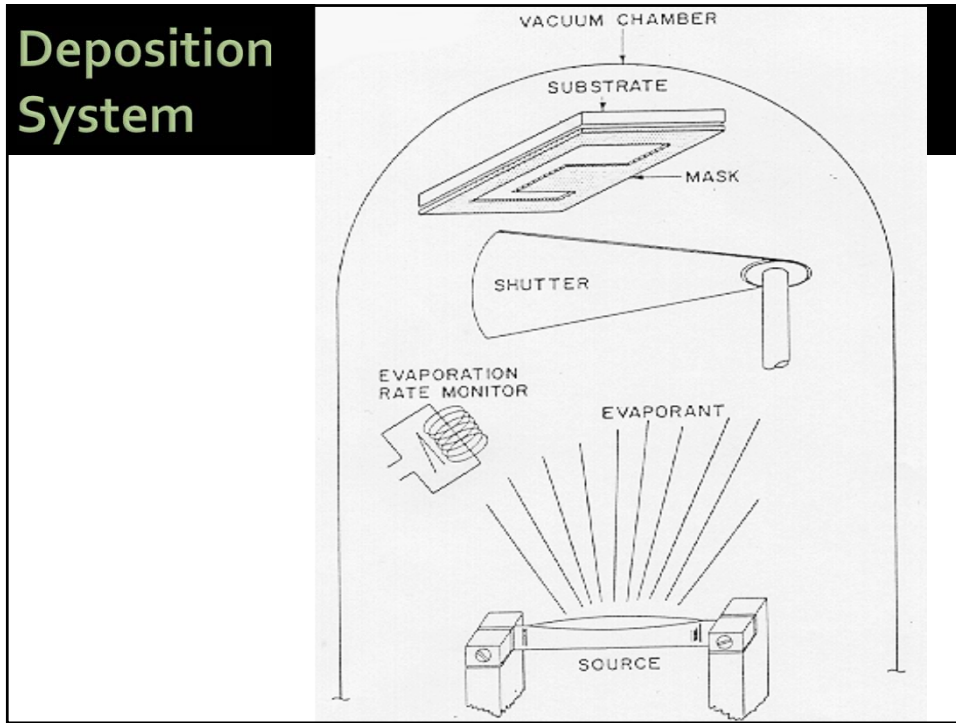
Figure 12.1 A simple diffusion-pumped evaporator showing vacuum plumbing and the location of the charge-containing crucible and the wafers.

5/14/2012

ECE 416/516 Spring 2011

8

Deposition System



Equilibrium vapor pressure at the material surface

Sublimation from solid source
Evaporation from molten source

$$P_e = 3 \times 10^{12} \sigma^{3/2} T^{-1/2} e^{\Delta H_v / NKT}$$

where σ = surface tension

ΔH_v = enthalpy of evaporation

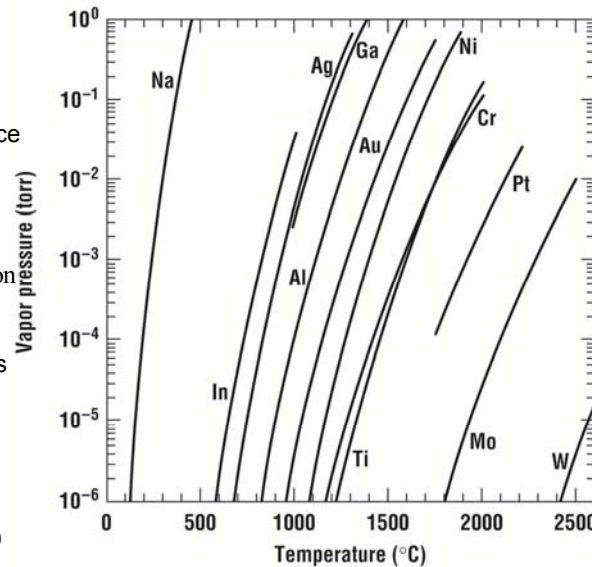
N = Avagadro's number

But equation gives large errors for small variations in ΔH_v , so usually use experimental data

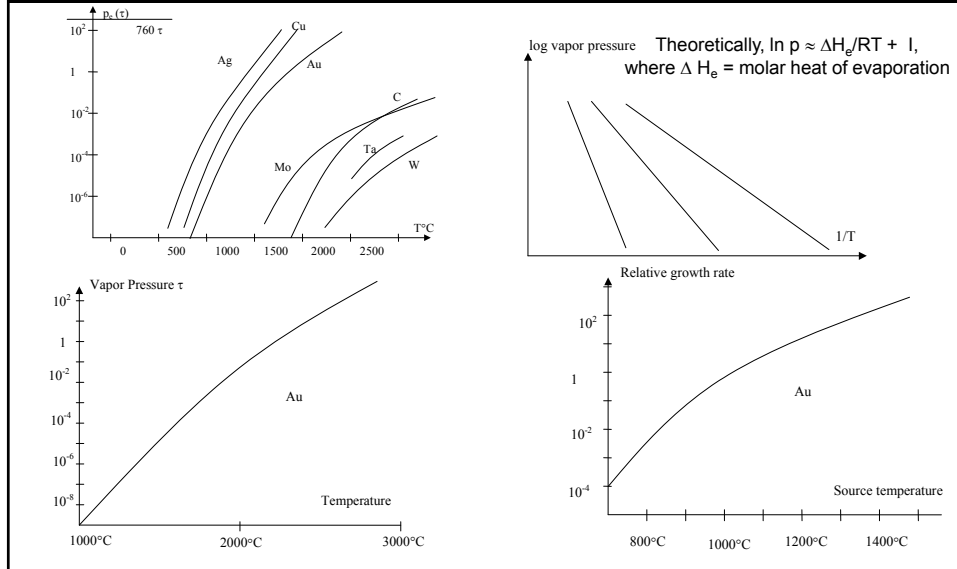
Deposition at VP ~ 10mtorr
e.g. Ag, Au vs Ti, Mo, W, (Ta)
(refractory metals)

Also: Al

Figure 12.2 Vapor pressure curves for some commonly evaporated materials (data adapted from Alcock et al.).



Vapor Pressure & Growth Rate



Evaporation Rate

Molecular Impingement flux $J = p / (2\pi mkT)^{1/2}$

(see back)

p = partial pressure

m = molecular mass

J in molecules / unit area / unit time

J = evaporation rate at equilibrium

Non-equilibrium : $T_e \gg T_{\text{amb}}$

$p_e \gg p_n$ background

$J_e = \alpha_e [p_e(T_e) - p_n] / (2\pi mkT)^{1/2}$

α_e = evaporation coefficient

Deposition rates

Number gas molecules crossing plane/unit area.unit time

$$J_n = \sqrt{\frac{P^2}{2\pi mkT}} \text{ gives mass evaporation rate } R_{ME} = \sqrt{\frac{m}{2\pi kT}} P_e$$

$$\text{so mass loss rate at crucible } R_{ML} = \int \sqrt{\frac{m}{2\pi kT}} P_e dA = \sqrt{\frac{m}{2\pi k}} \int \frac{P_e}{\sqrt{T}} dA$$

$$R_{ML} \approx \sqrt{\frac{m}{2\pi k}} \frac{P_e}{\sqrt{T}} A, \text{ for } T \text{ uniform and } A \text{ constant}$$

5/14/2012

ECE 416/516 Spring 2011

13

Example 12.1: Hemispherical water droplet, radius $r_0=1\text{mm}$, in vacuum at 300K. How long to evaporate?

No of water molecules $N = \frac{1}{2} \frac{4}{3} \pi r^3 \rho \frac{1}{m}$

so $\frac{dN}{dt} = 2\pi r^2 \frac{dr}{dt} \frac{\rho}{m}$

and $J = \frac{1}{A} \frac{dN}{dt} = 2\pi r^2 \frac{dr}{dt} \frac{\rho}{m} / \frac{1}{2} 4\pi r^2 = \sqrt{\frac{P_e^2}{2\pi mkT}}$

so $\frac{dr}{dt} = \frac{P_e}{\rho} \sqrt{\frac{m}{2\pi kT}} = \text{constant with time}$

At 300K, P_e is 27 torr = 3600 Pa, and

$$t = \frac{r_0}{dr/dt} = \frac{r_0 \rho}{P_e} \sqrt{\frac{2\pi kT}{m}} = 35m \text{ sec}$$

Note: Latent heat of evaporation would lower T with time, also reducing P_e .

5/14/2012

ECE 416/516 Spring 2011

14

Point Source Deposition

Total mass evaporated = M_e

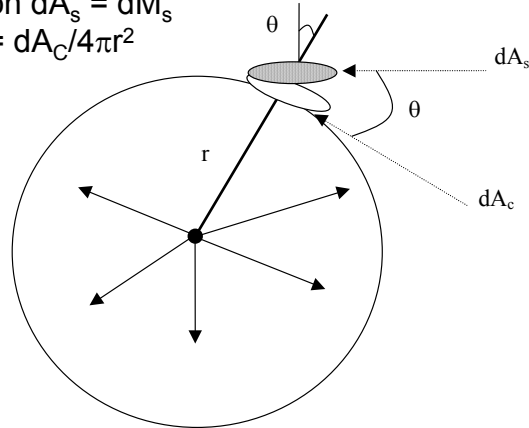
Mass deposited on $dA_s = dM_s$

$$dM_s/M_e = dA_c/4\pi r^2$$

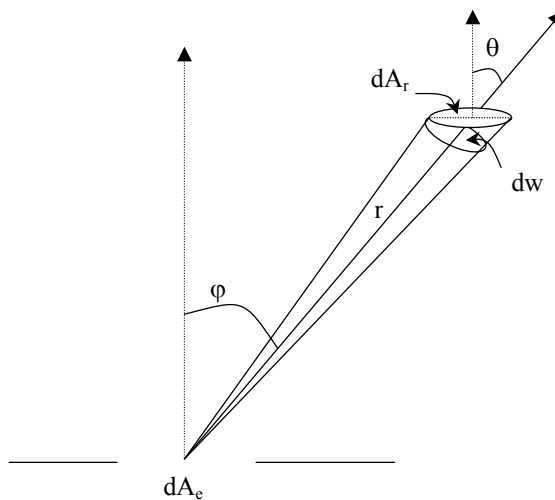
dA_c is projection of dA_s ,

$$dA_c = dA_s \cos \theta$$

$$\therefore dM_s/dA_s = M_e \cos \theta / 4\pi r^2$$



Surface Source Deposition (Knudsen source-narrow aperture)



Deposition Rates

a) **Point source**

$$F_k^P = \frac{R_{\text{evap}}}{\Omega r^2}$$

$$v = \frac{R_{\text{evap}}}{\Omega N r^2} \cos \theta_k$$

b) **Small planar surface source**

$$F_k^P = \frac{R_{\text{evap}}}{\pi r^2} \cos^n \theta_i$$

$$v = \frac{R_{\text{evap}}}{\pi N r^2} \cos^n \theta_i \cdot \cos \theta_k$$

- The evaporation source can be considered either a point source or as a small area surface source (latter is more applicable to most evaporation systems).
- Ω is the solid angle over which the source emits (4π if all directions, 2π if only upwards); N is the density of the material being deposited.
- The outward flux F_k^P from a point source, is independent of θ_i , while the outward flux from a small area surface source, varies as $\cos^n \theta_i$.

a. Uniform (isotropic) emission from a point source

b. Ideal cosine emission from a small planar surface source.
($n = 1$ in $\cos^n \theta$ distribution)

c. Non-ideal, more anisotropic emission from a small planar surface source.
($n > 1$ in $\cos^n \theta$ distribution)

5/14/2012 ECE 416/516 Spring 2011 17

Cosine Law in Practice

cos ϕ dependence: In practice $\cos^n \phi$

$$\therefore dM_r/dA_r = M_e (n+1) \cos^n \phi \cos \theta / 2\pi r^2$$

$$\rightarrow M_e \cos \phi \cos \theta / \pi r^2 \text{ for } n=1$$

Planetary Substrate Holder

$$\cos \vartheta = \cos \theta$$

$$= (r/2)/r_0$$

$$\therefore dM_r/dA_r = M_e (r/2r_0)^2 / \pi r^2$$

$$= M_e / 4\pi r_0^2$$

Point source

Arbitrary geometry
(A)

If $\cos \theta = \cos \phi = R / 2r$
then deposition rate

$$R_d = \text{Evap rate} \times \frac{\cos \theta \cdot \cos \phi}{\pi \rho R^2}$$

$$= \sqrt{\frac{m}{2\pi k}} \frac{P_e}{\sqrt{T}} A \frac{1}{\pi \rho R^2} \frac{R^2}{4r^2}$$

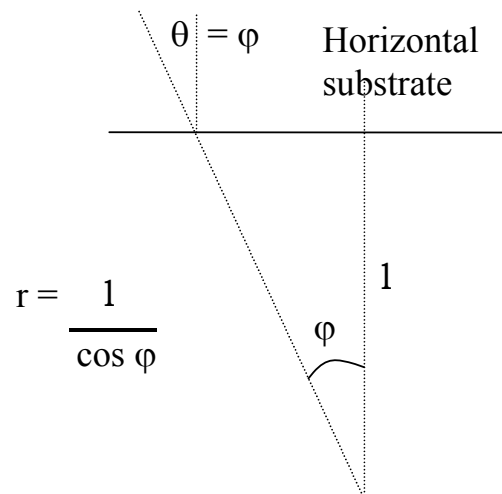
$$= \sqrt{\frac{m}{2\pi k}} \frac{P_e}{\rho \sqrt{T}} \frac{A}{4\pi r^2}$$

(Planetary deposition,
independent of $\theta = \phi$)

Spherical surface ($\theta = \phi$)
(B)

Figure 12.3 The geometry of deposition for a wafer (A) in an arbitrary position and (B) on the surface of a sphere.

Horizontal Substrate Holder



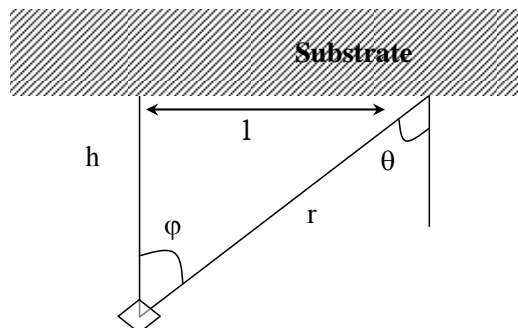
Film Uniformity: Point Source

Film thickness $d = dM_r / \rho dA_s$

For point source $d = M_e \cos \theta / 4 \pi \rho r^2$

$$= M_e h / 4 \pi \rho r^3$$

$$= M_e h / 4 \pi \rho (h^2 + l^2)^{3/2}$$

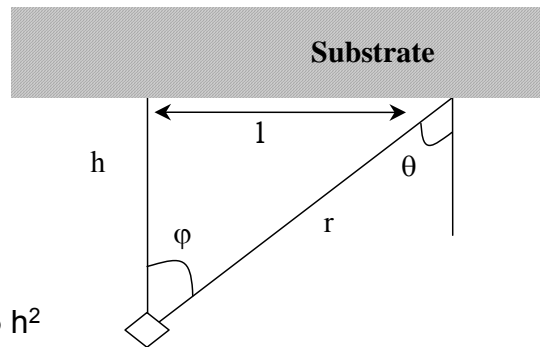


& thickest point $d_0 = M_e h / 4 \pi \rho h^3$

$$\therefore d/d_0 = h^3 / (h^2 + l^2)^{3/2} = 1 / [1 + (l/h)^2]^{3/2}$$

Film Uniformity: Surface Source

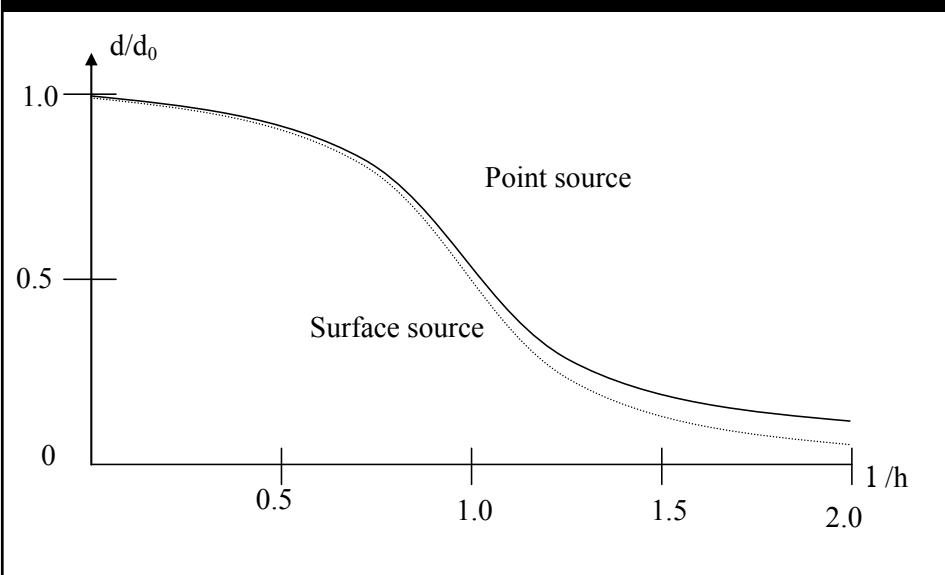
$$\begin{aligned}
 \text{Film thickness } d &= M_e \cos \phi \cos \theta / \pi \rho r^2 \\
 &= (M_e / \pi \rho r^2)(h/r)(h/r) \\
 &= M_e h^2 / \pi \rho r^4 \\
 &= M_e h^2 / \pi \rho (h^2 + l^2)^2
 \end{aligned}$$



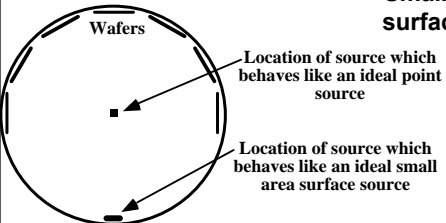
& for $d_0 = M_e / \pi \rho h^2$

$$\therefore d/d_0 = h^4 / (h^2 + l^2)^2 = 1 / [1 + (l/h)^2]^2$$

Film Uniformity Comparison



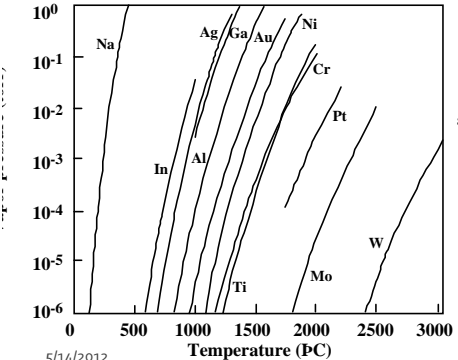
- Uniform thickness - use spherical wafer holder.
- Point source: put source at center of sphere.
- Small surface source: put source on inside surface of sphere (compensates for $\cos^n \theta_i$).



Location of source which behaves like an ideal point source

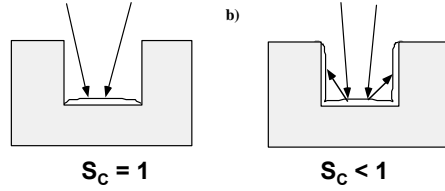
Location of source which behaves like an ideal small area surface source

- With evaporation:
 - Can evaporate just about any element.
 - Difficult to evaporate alloys and compounds
 - Sticking coefficient $S_c = F_{\text{reacted}}/F_{\text{incident}}$
 - Step coverage is poor (line of sight and $S_c \approx 1$).
 - Rarely used today.



Evaporation Rate (gm/sec)

Temperature (°C)



a) $S_c = 1$

b) $S_c < 1$

$R_{\text{evap}} = 5.83 \times 10^{-2} A_s (m/T)^{1/2} P_e \text{ gm/sec}$

5/14/2012 25




Figure 12.10 A commercial evaporator. Inset shows a planetary (photographs courtesy of CHA Industries).

5/14/2012 ECE 416/516 Spring 2011 26

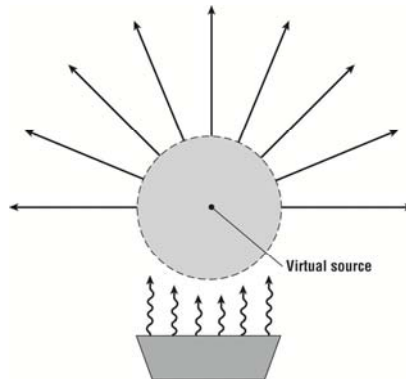


Figure 12.4 At high deposition rates, the equilibrium vapor pressure of the charge puts the region just above the crucible into viscous flow, creating a virtual source up to 10 cm above the top of the crucible.

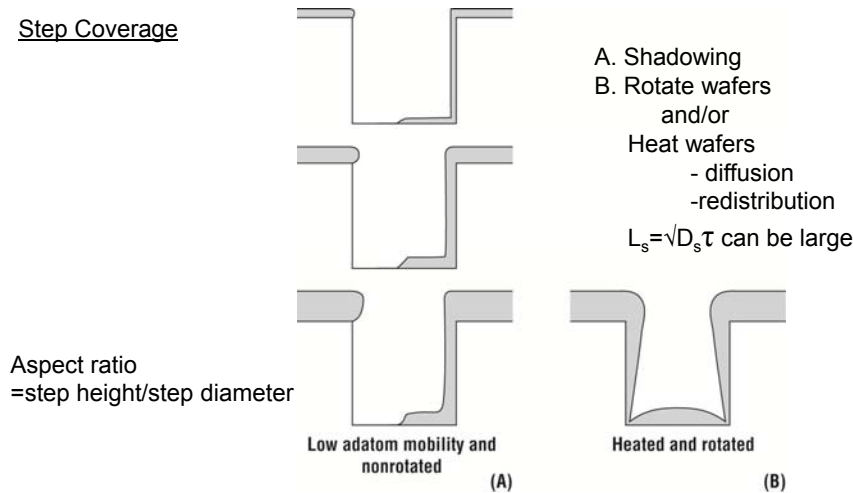
High rate depositions → high molecular density in the vapor
 Hence vapor can condense into droplets
 Hence deposit slowly → possible contamination

5/14/2012

ECE 416/516 Spring 2011

27

Step Coverage



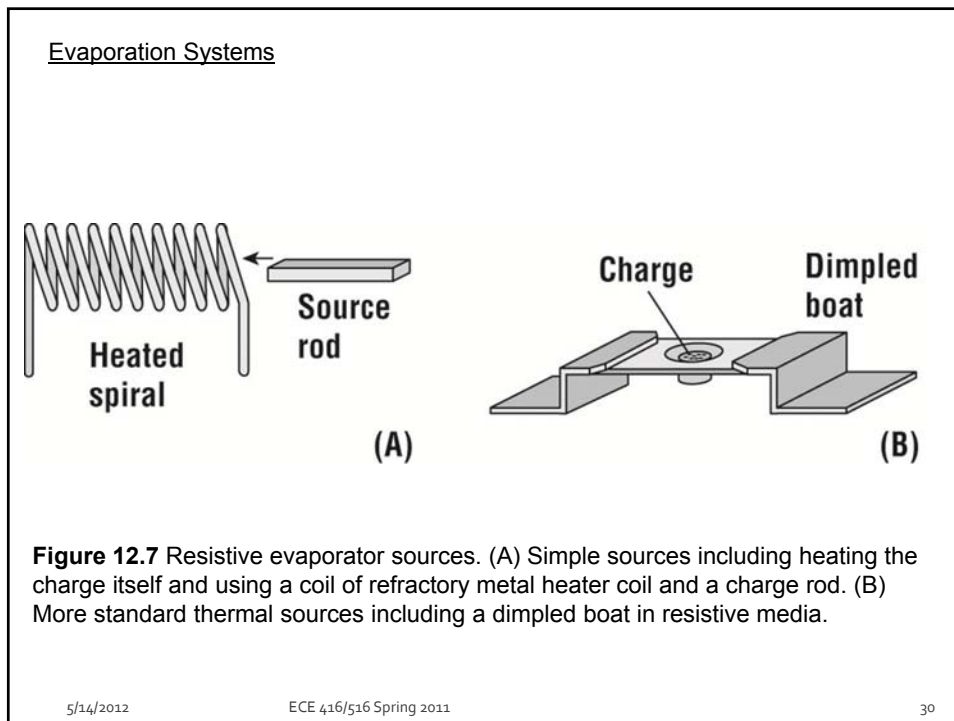
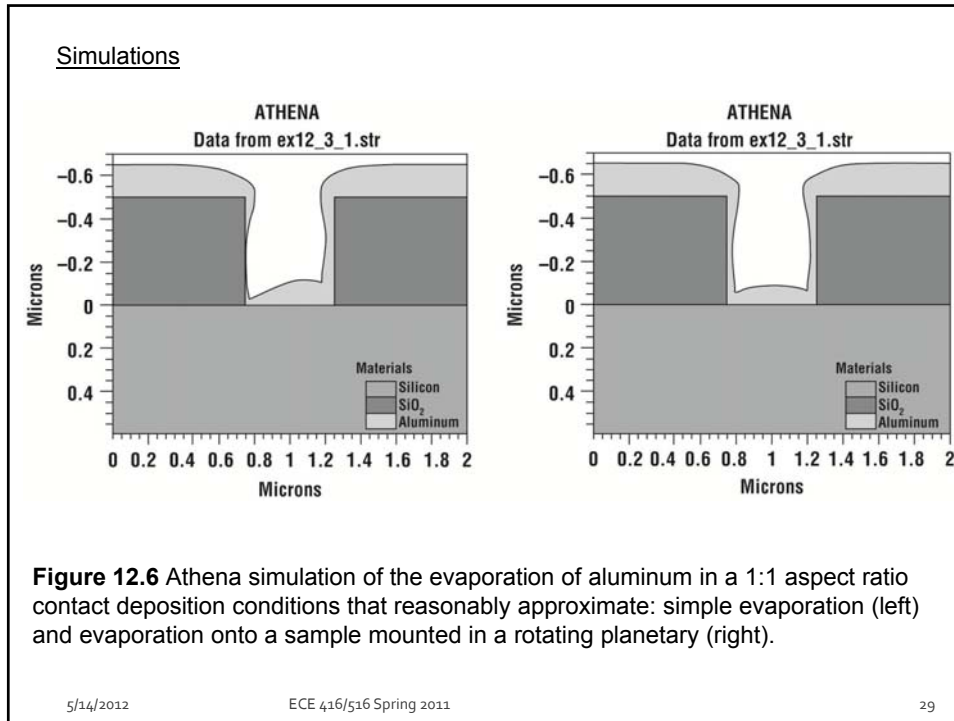
Aspect ratio
 =step height/step diameter

Figure 12.5 (A) Time evolution of the evaporative coating of a feature with aspect ratio of 1.0, with little surface atom mobility (i.e., low substrate temperature) and no rotation. (B) Final profile of deposition on rotated and heated substrates.

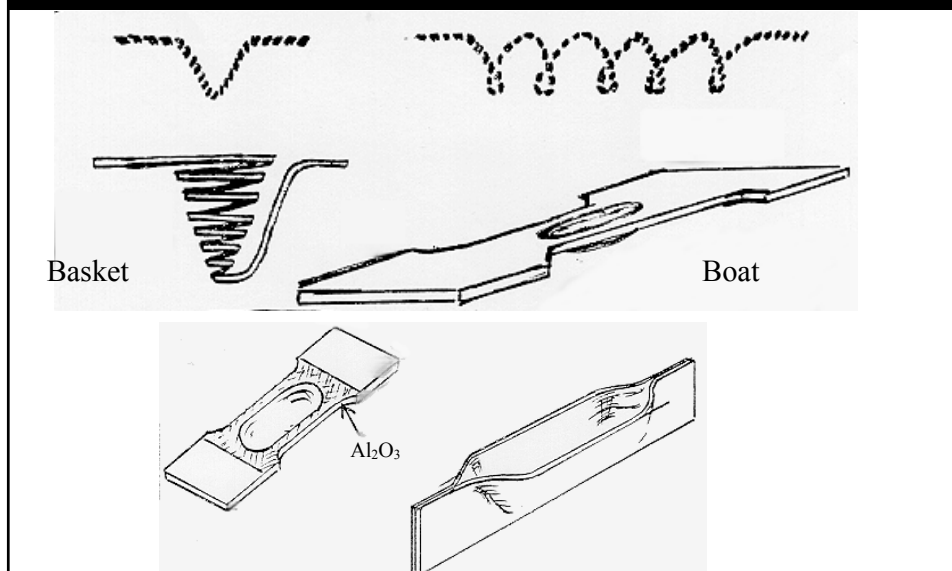
5/14/2012

ECE 416/516 Spring 2011

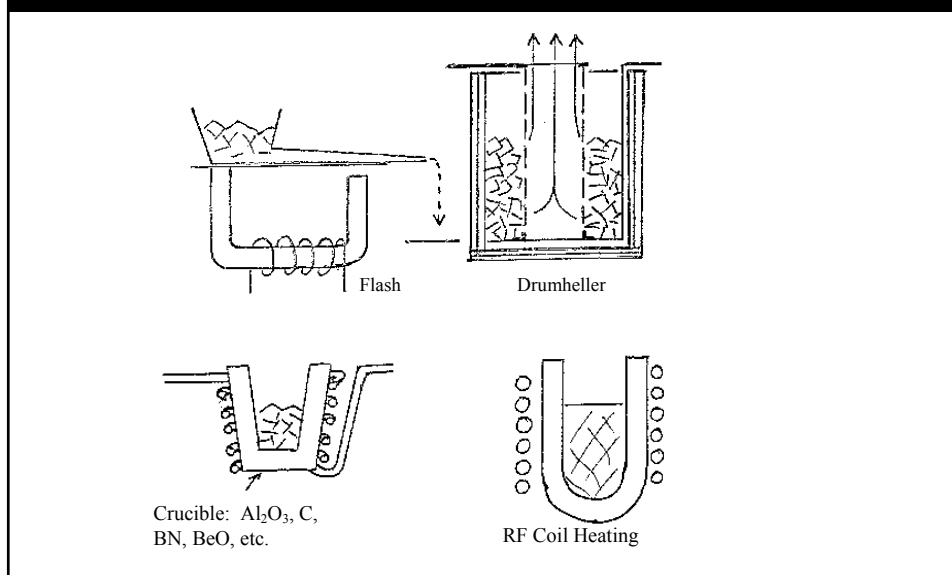
28

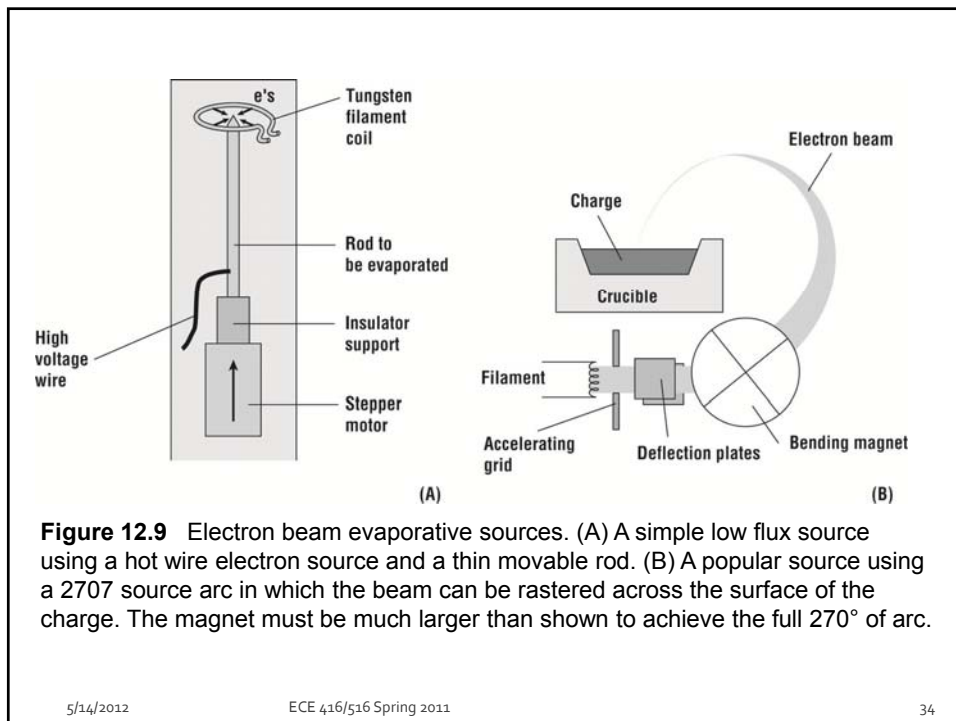
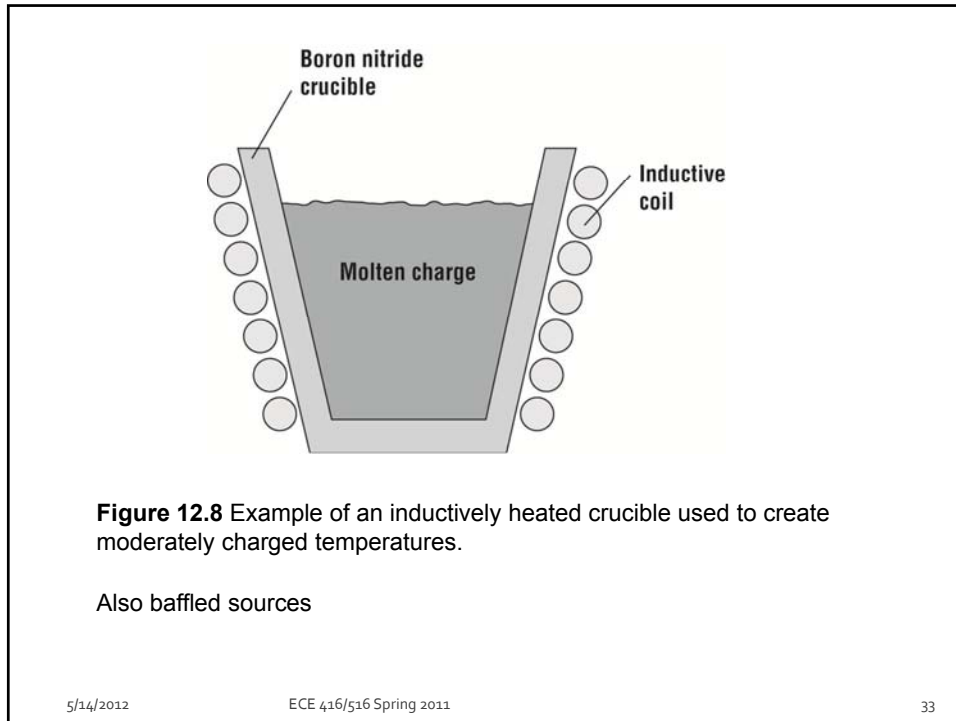


Evaporation Sources #1

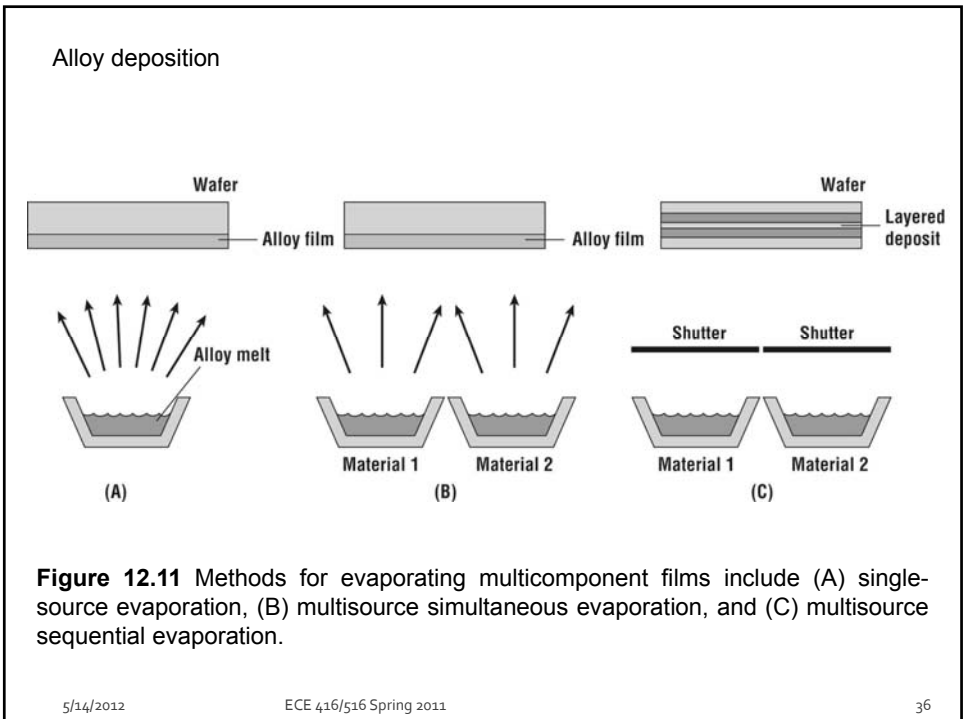
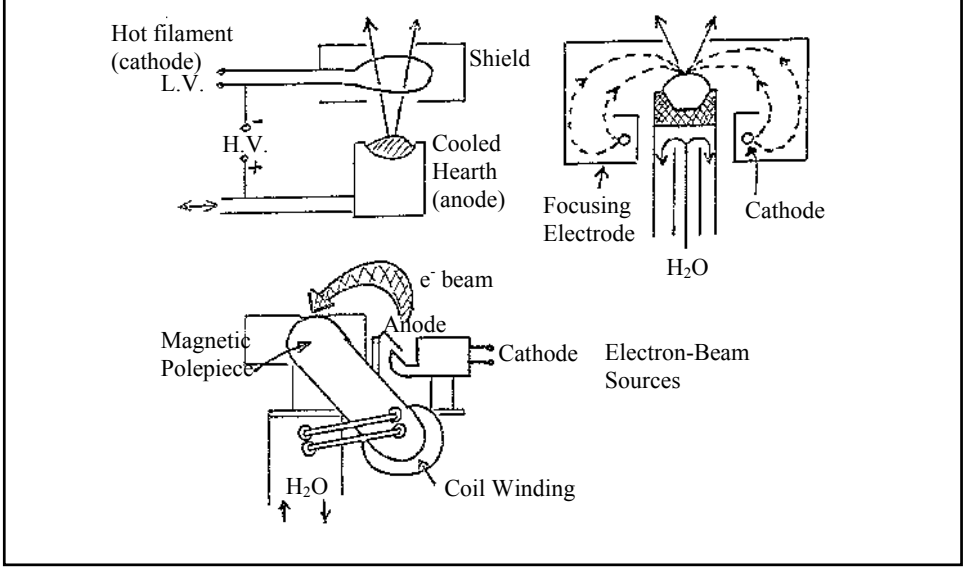


Evaporation Sources #2





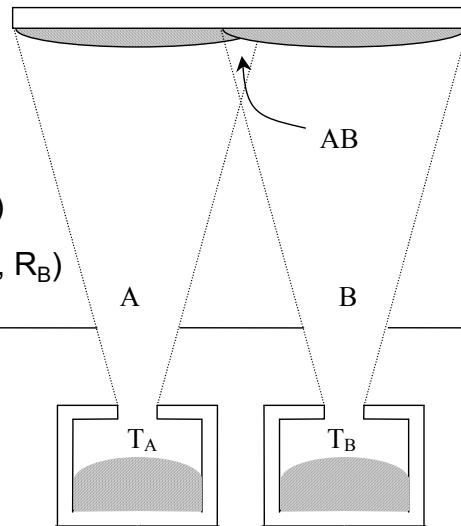
Evaporation Sources #3



Alloy Deposition Control

Composition control:

- (a) Source temperature (MBE)
- (b) Twin monitors (Control R_A , R_B)
- (c) Master-Slave monitors
(Control $R_B = kR_A$)



Alloy Deposition

Single Source e.g. NiCr

Vapor pressure difference

Equilibrium

Film composition function of
source temp, time

Flash Evaporation

Intermetallics (GaAs, PbTe, InSb, etc.)

Cermets

Sputter

Impurity Contamination

Relate to deposited evaporant flux

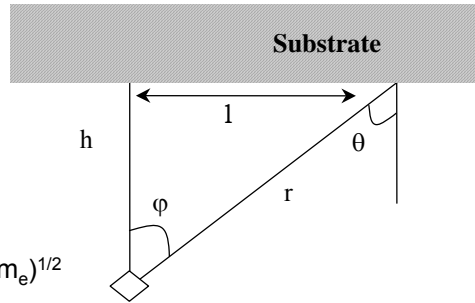
$$J_e = p_e / (2\pi m_e k T_e)^{1/2}$$

& at horizontal substrate (surface source)

$$J' = J_e A_e \cos^4 \phi / \pi h^2$$

(valid only for small A_e)

$$= J_e A_e (h^2 / \pi l^2)$$



Contaminant in source

$$J_c = p_c / (2\pi m_c k T_e)^{1/2}$$

i.e. contamination $(p_c/p_e)/(m_c/m_e)^{1/2}$

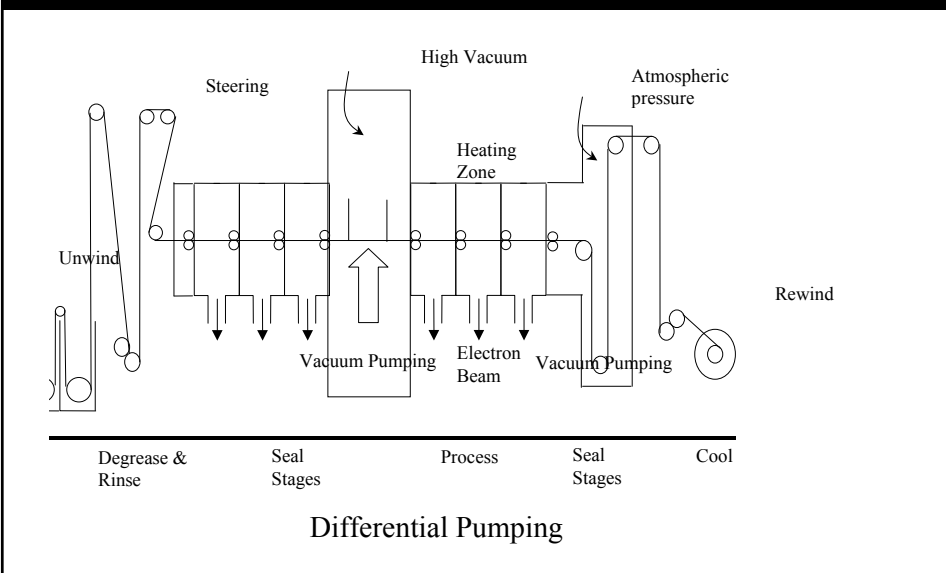
Background contamination

$$J = p_p / (2\pi m k T)^{1/2}$$

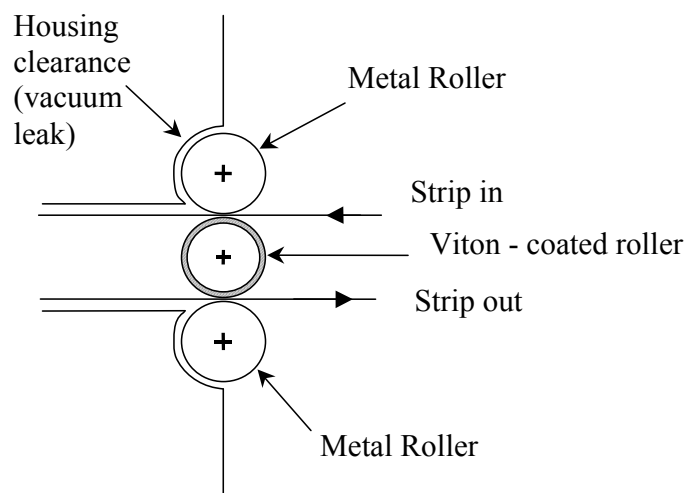
p_p partial pressure of contaminant,
molecular mass m,
ambient temperature T.

Uniform across substrate.

Roll Coater #1

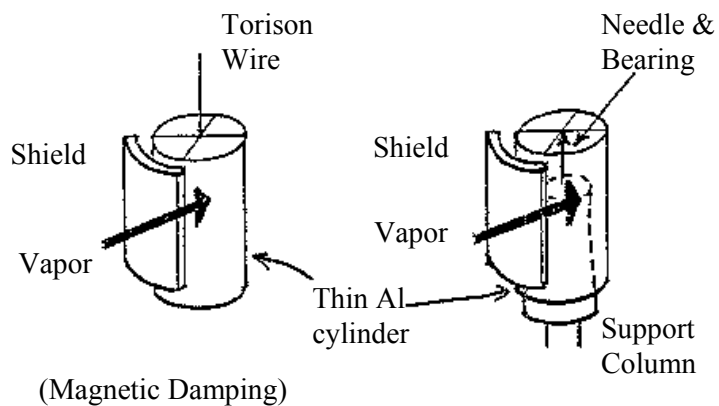


Roll Coater #2



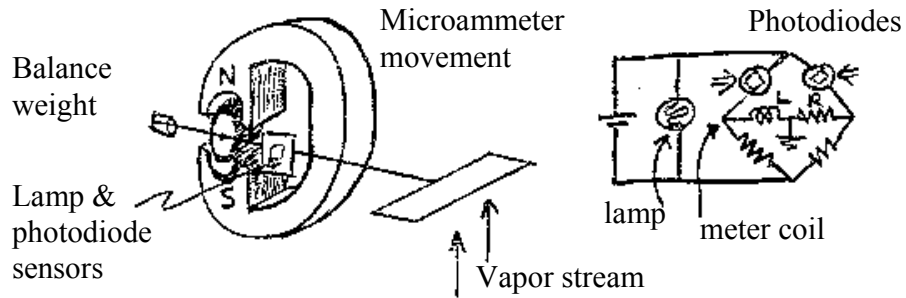
Deposition Rate Monitors 31

Particle impingement



Deposition Rate Monitors #2

Mechanical Microbalance measures deposited mass.

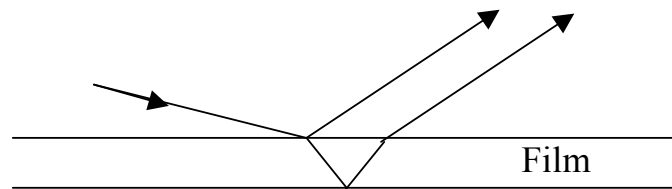


(see also Quartz crystal)

Deposition Rate Monitors #3

Optical Monitors

- (a) Reflectance
- (b) Transmittance
- (c) Absorption
- (d) Interference (oscillatory with thickness)



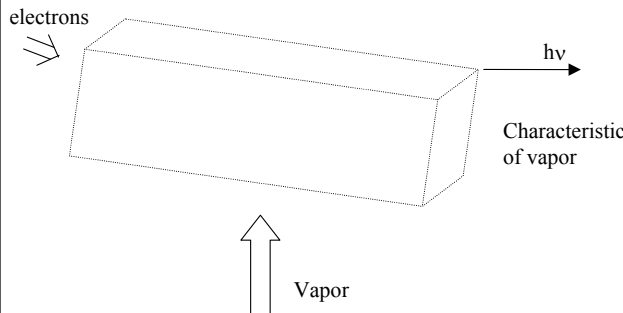
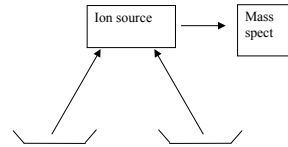
Resistance

Substrate

Deposition Rate Monitors #4

Ionization gauge monitors

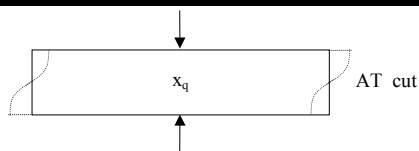
Mass spectrometry
(especially for alloy
deposition)



EIES: electron
induced emission
spectroscopy

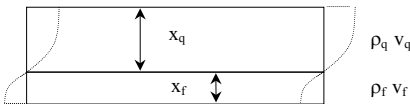
Detector for each
species, no build up

Quartz Crystal Monitor



Thickness shear oscillation mode:

$$x_q = \lambda/2 = v_q/2f_q = 1/2 v_q \tau_q$$



$$\Delta f_q/f_q \approx -\Delta m_f/m_q \rightarrow \Delta f \approx - (m_f/m_q) f_q$$

for $m_f/m_q \leq 0.01$

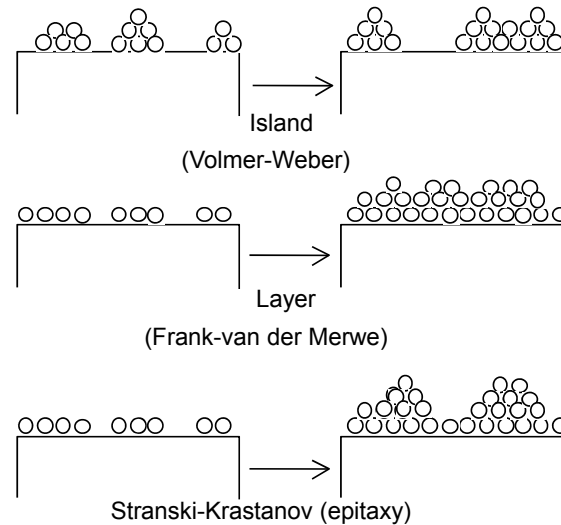
Write $\Delta f \Rightarrow -m_f * f_q / (\rho_q x_q) = -m_f * 2f_q^2 / (\rho_q v_q)$
Only time AT f_q (single frequency)

write $dm_f = -(\rho_q v_q / 2 f_c^2) df_c$
& integrate $\int_{f_c}^{f_q} dm_f = -\rho_q v_q / 2 \int_{f_c}^{f_q} df_c / f_c^2$

$$m_f = \rho_q v_q / 2 (1/f_c - 1/f_q)$$

$$\therefore x_f = (v_g \rho_g / 2 \rho_f) (\tau_c - \tau_q)$$

Thin Film Growth Modes



Homogeneous Nucleation: Vapor Pressure

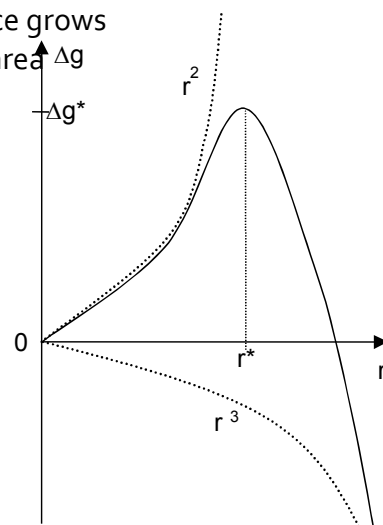
- Spontaneous nucleation in gas phase
 - no surface, dust, charge, etc.
 - undesirable in practice -> polycrystals
- If solid has vapor pressure P_∞ & pressure of vapor above solid is P
 - if $P = P_\infty$, vapor does not condense, solid does not evaporate
 - vapor condenses if $P > P_\infty$

Homogeneous Nucleation: Gibbs Free Energy

- $PV = (NR)T = (nk)T$
 - N = number moles, R = gas constant
 - n = number molecules, k = Boltzmann constant
- When vapor condenses:
 - Energy change when $P \rightarrow P_\infty = \int V dP$
 - $= nkT \int_{P_\infty}^P dP/P$
 - $= -nkT \ln P/P_\infty = \Delta G_v$
 - $\Delta G_v =$ Gibbs Free Energy of Formation
- As atoms add to nucleus,
nucleus grows with release of free energy
- Note: ΔG_v negative

Homogeneous Nucleation: Critical Nucleus

- As nucleus grows, solid-vapor interface grows
 \therefore increase in free energy σ /unit area
- Total increase in energy:
- $\Delta G_{\text{homo}} = (4/3)\pi r^3 \Delta G_v + (4\pi r^2)\sigma$
Max at $r^* = -2\sigma/\Delta G_v$
- $\Delta G^* = (16\pi/3)(\sigma^3/\Delta G_v^2)$



Homogeneous Nucleation: Growth

For nucleus $r < r^*$, ΔG decreases by breaking up.

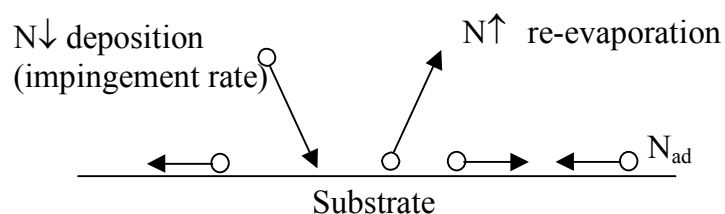
For nucleus $r > r^*$, ΔG decreases by growth.

If P/P_∞ large, i.e. high supersaturation,
 $|\Delta G_v|$ incr. $\rightarrow r^*$ decr.

Note: This is classical bulk thermodynamic approach. As $r^* \rightarrow r_{\text{atomic}}$, cannot use bulk values of σ , surface concept, etc.

Heterogeneous Nucleation

- Introduce substrate, dust, etc. into vapor
- Consider adatoms on substrate, N_{ad} /unit area



Heterogeneous Nucleation: Residence Time

- Re-evaporation probability: $W = \nu \exp(Q_{ad}/kT)$
where Q_{ad} = binding energy to substrate (negative)
- Re-evaporation rate $N \uparrow = N_{ad} \nu \exp(Q_{ad}/kT)$
- Steady State: $N \uparrow = N \downarrow$ gives $N_{ad} = (N \downarrow / \nu) \exp(-Q_{ad}/kT)$
- Residence time $\tau = W^{-1} = \nu^{-1} \exp(Q_{des}/kT)$
where Q_{des} = desorption energy (positive)
and $Q_{ad} = -Q_{des}$
& $W = \text{Re-evaporation probability}$
 $= \tau^{-1} = \nu \exp(-Q_{des}/T)$

Heterogeneous Nucleation: Adsorption Rate

Note: Assumes only adatom population with no further interaction. If $N \downarrow \rightarrow 0$ (deposition stopped), $N_{ad} \rightarrow 0$, i.e. all eventually re-evaporate.

Adsorption Rate: $dN_{ad}/dt = N \downarrow - N \uparrow = N \downarrow - N_{ad} / \tau$

Solve: $dN_{ad} / (N \downarrow \tau - N_{ad}) = dt / \tau$ for $N_{ad} = 0$ at $t = 0$,

gives: $N_{ad}(t) = N \downarrow \tau (1 - \exp(-t/\tau))$

$\rightarrow N \downarrow \tau$ for $\tau \ll t$

i.e. independent of time for weak physical adsorption.

(compare steady state result previous slide)

$\rightarrow N \downarrow t$ for $\tau \gg t$

i.e. defines "complete condensation" for strong adsorption or initial transient.

Heterogeneous Nucleation: Surface Diffusion

Surface diffusion of adatom ---> moves X from pt. of impact
 $X = (2D\tau)^{1/2} = (2D)^{1/2} v^{-1/2} \exp(-Q_{ad}/2kT)$

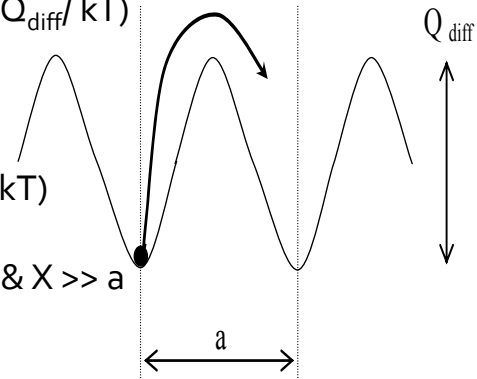
where D = surface diffusivity

$$= a^2 v \exp(-Q_{diff}/kT)$$

$$X = z^{1/2} a \exp(-((Q_{diff} + Q_{ad})/2kT))$$

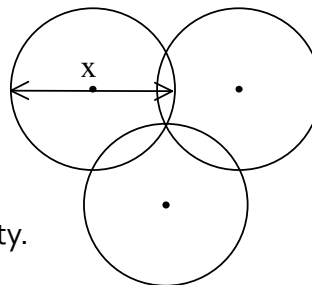
$|Q_{ad}| > Q_{diff}$ always

$|Q_{ad}| - Q_{diff} \gg kT$ typically & $X \gg a$



Heterogeneous Nucleation: Capture Distance

When adjacent nuclei separation $< X$,
 no further nuclei created
 all atoms join existing nuclei.

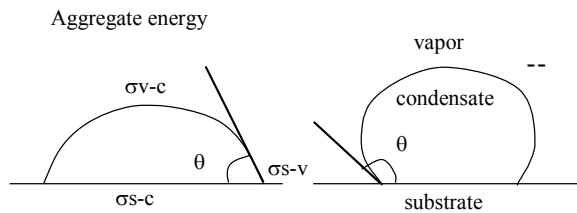


\therefore Can find a saturation nucleation density.

Capillary Model

For island clusters with $|Q_{ad}| \gg kT$ (cold substrate/metal on metal)

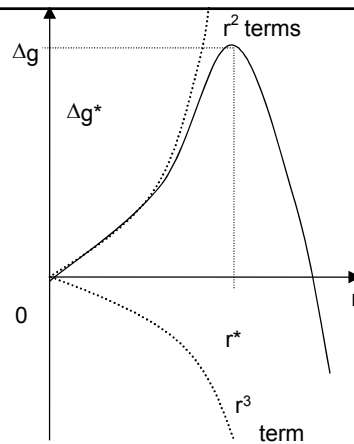
$N \uparrow$ small & N_{ad} large
Interatomic collisions
>clustering.



$$\Delta G = a_3 r^3 \Delta G_v + a_1 r^2 \sigma_{v-c} + a_2 r^2 \sigma_{s-c} - a_2 r^2 \sigma_{s-v}$$

where $\Delta G_v =$ Free energy of condensation (negative)
 $= (kT/V) \ln N \downarrow / N \uparrow$ ($V =$ molecular volume)

Critical Cap Size



Differentiate

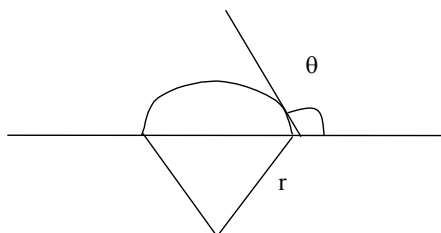
$$\Delta G / \partial r = 3a_3 r^2 \Delta G_v + 2a_1 r \sigma_{v-c} + 2a_2 r (\sigma_{s-c} - \sigma_{s-v})$$

=> 0 at $r^* =$ critical radius

gives $\Delta G^* = [4(a_1 \sigma_{v-c} + a_2 \sigma_{s-c} - a_2 \sigma_{s-v})] / (27a_3^2 \Delta G_v^2)$

at $r^* = [-2(a_1 \sigma_{v-c} + a_2 \sigma_{s-c} - a_2 \sigma_{s-v})] / 3a_3 \Delta G_v$

Spherical Cap



Also: For spherical cap nucleus, contact angle θ
 [θ determined by σ 's, ΔG_v for min tot ΔG

$$\text{i.e. } \theta = f^{\Delta}(\sigma_{v-c}, \sigma_{s-c} - \sigma_{s-v}, \Delta G_v)$$

gives: $\Delta G^* = [(4\pi \sigma_{v-c}^3) / 3\Delta G_v^2] (2 + \cos \theta)(1 - \cos \theta)^2$

$$\text{at } r^* = -2 \sigma_{v-c} / \Delta G_v$$

No. of monomers in critical cluster $i^* = (a_3 r^{*3} / V)$

Data: Surface Energies

Ag at	1173k	$\sigma_{c-v} = 1140 \text{ erg/cm}^2$	$\partial \sigma_1 / \partial T = -0.47 \text{ erg/cm}^2\text{k}$
Au	1276k	1450	$= -0.43$
Cu	1323k	1550	$= -0.46$
Sn	488k	685	
(from creep rates at melting point)			
Al		1157	
Cd		743	
Fe		1520	
Pb		528	
Mg		643	
Zn		932	
(from liquid surface tensions at melting point)			
glass		250-360	
Polymers(non-polar)		<100	
Polymers(polar)		<300	
$\gamma \text{Al}_2\text{O}_3$		560	
CdO		500	
CuO		<760	
MgO		1400	
Mg(OH) ₂ cryst		330	
Sn ₂ O ₃		140	

"Total" energy (all above
are "free" energy).

Data: Adsorption Energy

			\underline{Q}_{ad}	\underline{Q}_D
Na	on	W	-2.73eV	
Rb		W	-2.60	
Cs		W	-2.80	0.61eV
Ba		W	-3.80	0.65
W		W	-5.83	1.31
Hg		Ag	-0.11	
Cd		Ag	-1.61	
Al		NaCl	-0.60	
Cu		glass	-0.14	
Hg		Hg		0.048

Capillary Example: #1

Ag on glass at 300k at 1A/sec.

$$\sigma_{c-v} = 1140 - 0.47(300-1173) \text{ at } 1173\text{k (temp correction)}$$

$$= 1550 \text{ ergs/cm}^2$$

$$\sigma_{s-c} = \sigma_{c-v} + \Delta G_{ad} \text{ <---- (-ve) Free energy of absorption}$$

$$Q_{ad} \sim 0.12\text{eV} \times 1.6 \times 10^{-19} \text{J/eV} \times 10^7 \text{ergs/J} / \pi(1.5 \times 10^{-8} \text{cm})^2$$

$$= 300 \text{ ergs/cm}^2$$

i.e. $\sigma_{sc} \sim 1550 - 300 = 1250 \text{ ergs/cm}^2$

$$\sigma_{s-v} = 300 \text{ ergs/cm}^2 \text{ (250 to 360)}$$

$$\Delta G_v = -1.9 \times 10^{11} \text{ ergs/cm}^3$$

Capillary Example: #2

Ag on glass at 300k at 1A/sec. (continued)

$$\Delta G_v = -1.9 \times 10^{11} \text{ ergs/cm}^3$$

$N \uparrow \sim 10^{-40} \tau$ from vapor pressure data

& $N \downarrow \sim 10^{-6} \tau$

$$\text{from } p(\tau) = (MT)^{1/2} / [3.5 \times 10^{22} A] (dN/dt) / \text{s.cm}^2$$

Assuming hemispherical cap i.e. $\theta = 90^\circ$,

$r^* \sim 0.22 \text{ nm}$ for Ag on glass

Similarly for W on glass, r^* even less

$$r^* \leq \text{atomic radius}$$

Can't use macroscopic concepts like surfaces

Spherical Cap: General Trends

a) Weak substrate binding, θ large
e.g. Au on glass

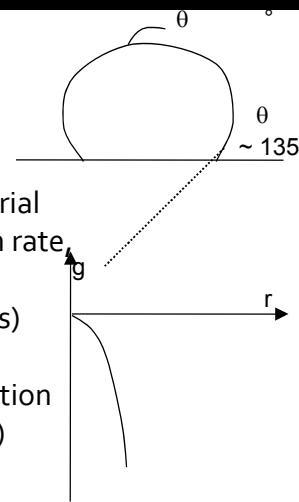
b) High supersaturation ratio
 $N \downarrow / N \uparrow \rightarrow$ small r^*
e.g. low v.p. material

(e.g. W, etc), cold substrate, high deposition rate,
strong substrate adhesion

Continuity reached early (many small islands)

c) ΔG_v large, $r^* \rightarrow 0$,
No nucleation barrier, monolayer formation
(or σ_{s-v} high, so $\sigma_{c-v} + \sigma_{c-s} \sim \sigma_{s-v}$)

d) $(\partial r^* / \partial T)_{N \downarrow} > 0$
 $(\partial r^* / \partial N \downarrow)_T < 0$
but large $\Delta N \downarrow$ required for significant Δr^* .



Charge Effects on Nucleation

N.B. NO initial barrier to nucleation;
only barrier to growth.

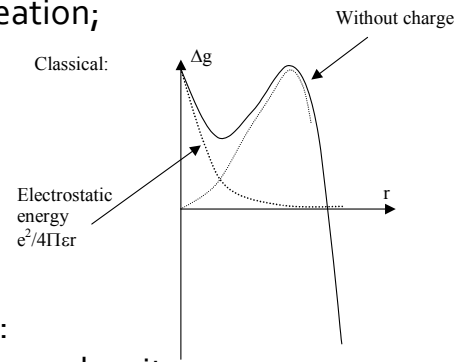
Experimental:

Substrate positively charged:

No effect
(random nucleation at
low deposition rates)

Substrate negatively charged:

Nucleation density \approx charge density



i.e. charge sites are nucleation (binding) sites.

Nucleation Rate

Adatom residence time $\tau = v^{-1} \exp -Q_{\text{des}}/kT$
where $N_{\downarrow} = N_A P / (2\pi MRT)$

$$N_{\text{ad}} = N_{\downarrow} \tau$$

Nucleation rate $N^R = N^* A^* \omega$

where $N^* = n_s \exp -\Delta G^*/kT$

n_s = nucleation site density

$$A^* = 2\pi r^* a_o \sin \theta$$

(area of circumferential belt of adjacent atoms)

Impingement rate onto area A^* , $\omega = \tau N_{\downarrow} D$, and

$$N^R = 2\pi r^* a_o \sin \theta P N_A / (2\pi MRT)^{1/2} n_s \exp(E_{\text{des}} - E_{\text{diff}} - \Delta G^*)/kT$$

=Rate of creation super critical nucleus

Critical Condensation

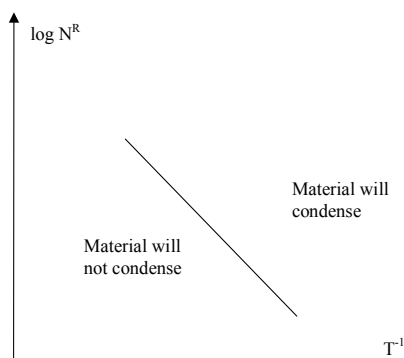
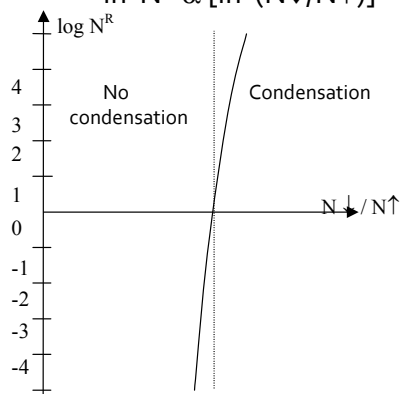
Note : $N^R \propto \exp - \Delta G^*/kT$

& $\Delta G^* \propto \Delta G_v^{-2}$

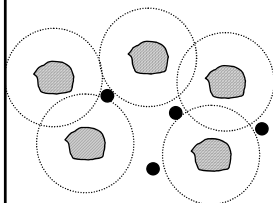
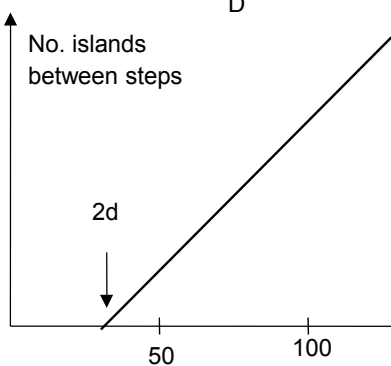
& $\Delta G_v \propto \ln(N\downarrow/N\uparrow)$

$\ln N^R \propto [\ln (N\downarrow/N\uparrow)]^2$

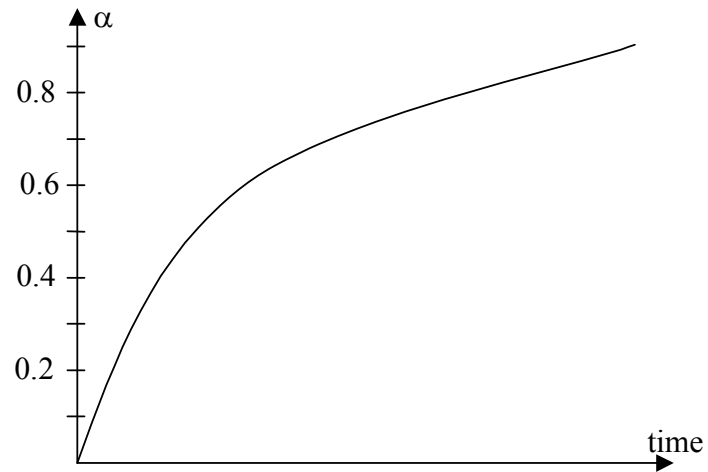
($N\downarrow/N\uparrow$ = super-saturation) ratio



Diffusion/Capture Distance



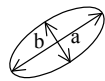
Condensation Coefficient



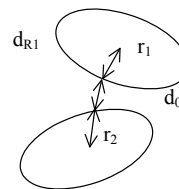
Island Shapes



Prolate ellipsoids



$$e^2 = 1 - (b/a)^2$$



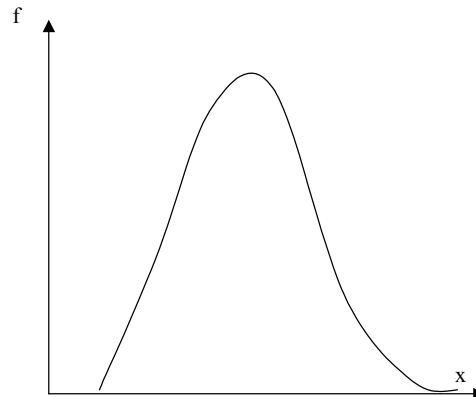
$$R_1 = r_1 + r_2 + d$$

CTC ETE

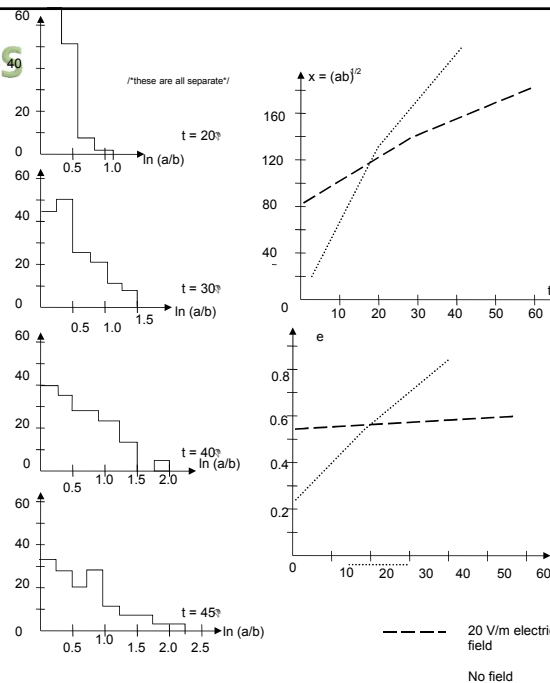
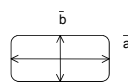
Island Shape distributions

Log-normal:-

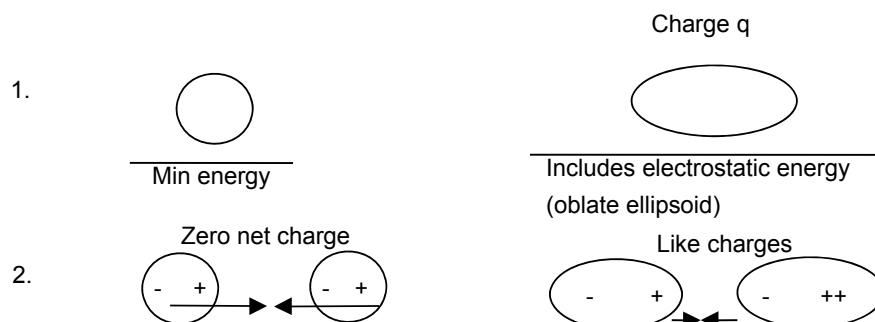
$$f_{LN}(x) = ((2\pi)^{1/2} \ln \sigma)^{-1} \exp -1/2 [(\ln(x/x_m)) / (\ln \sigma)]^2$$



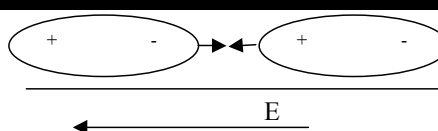
Eccentricities



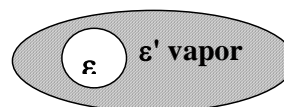
Charge Effects



Field Effects



1. Field enhanced coalescence



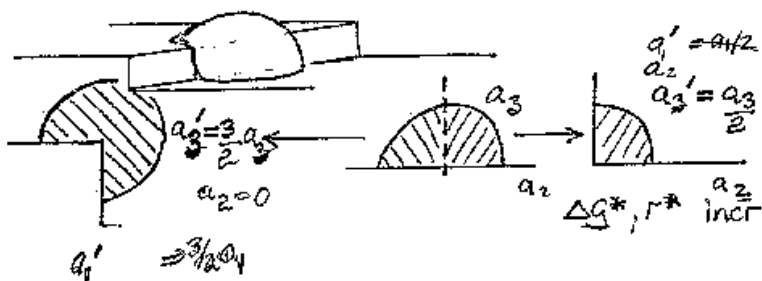
2. Nucleation

Field inhibited $\epsilon > \epsilon'$

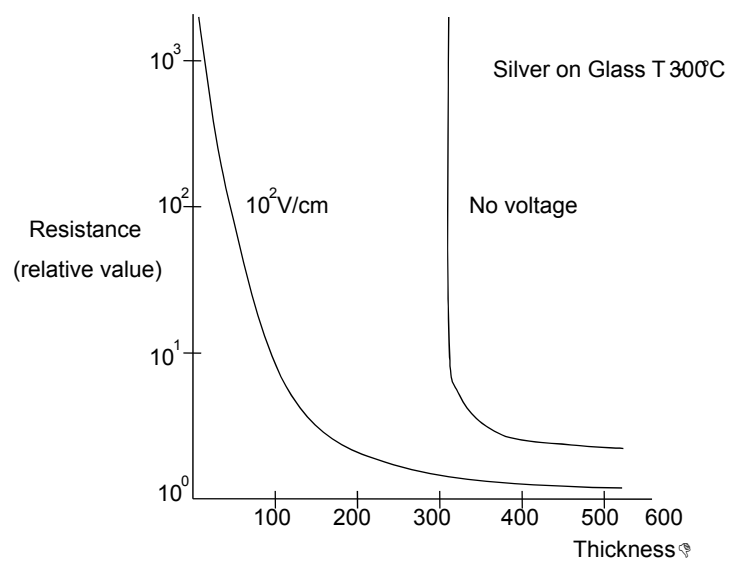
Field enhanced $\epsilon < \epsilon'$

$$\Delta = r^3 E^2 [((\epsilon' - \epsilon) \epsilon') / (2 \epsilon' + \epsilon)]$$

Substrate Defects

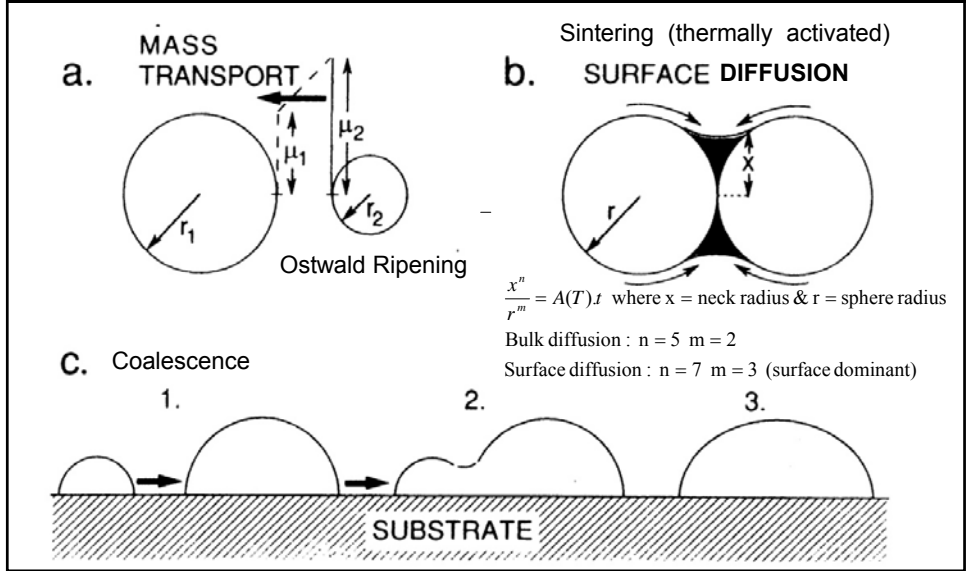


$\Delta G^*, r^*$ increase, but less atoms/critical nucleus



Experimental Field Effect

Coalescence (Ohring (2002))



Sputter Deposition

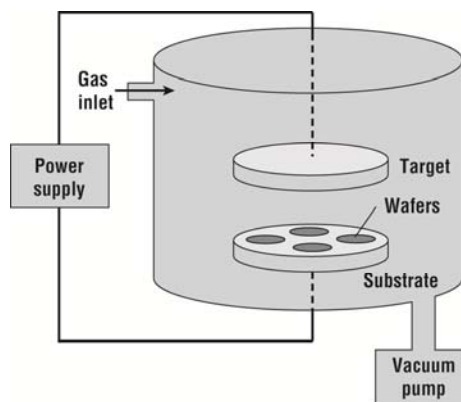
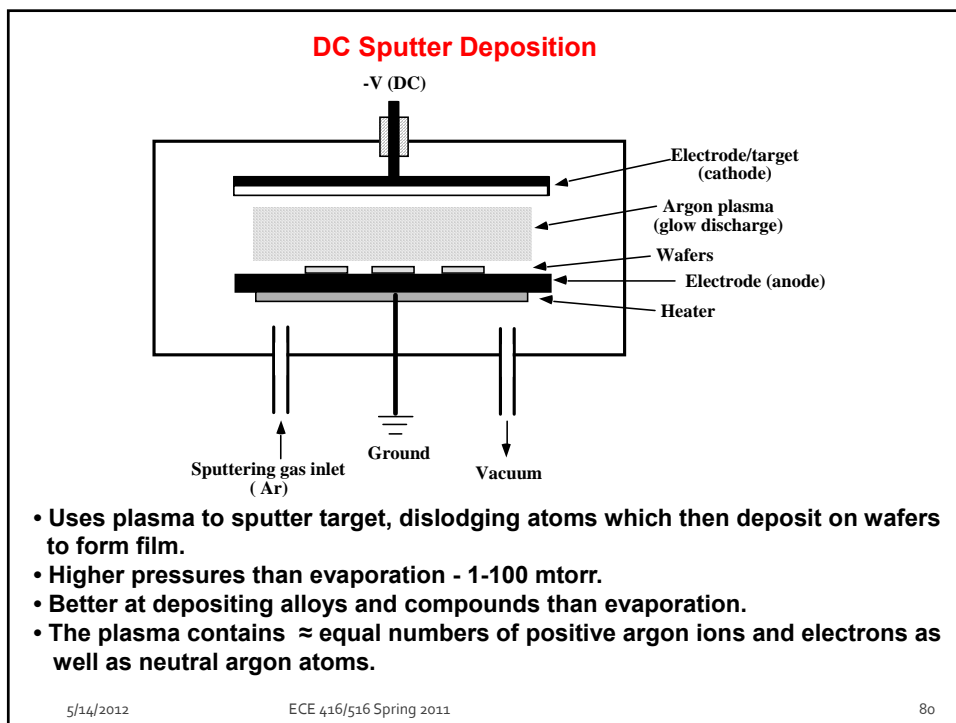
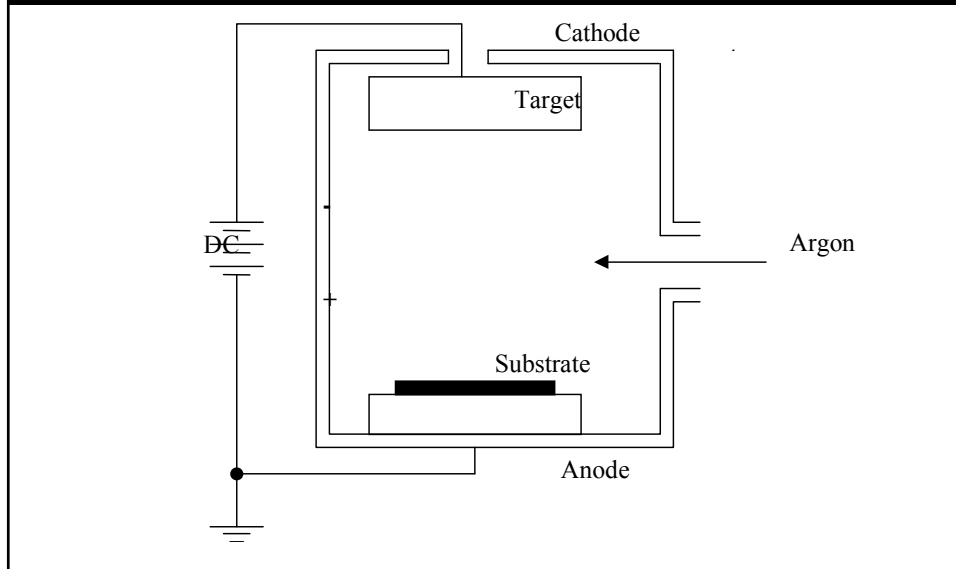


Figure 12.12 Chamber for a simple parallel-plate sputtering system.

DC Sputter Deposition



The diagram illustrates the components and processes of a sputtering system. At the top, a cross-section shows a Cathode (target) on the left, an Anode on the right, and Wafers positioned above the anode. The Cathode is connected to a negative DC voltage source (V_c). The Anode is grounded. The region between the cathode and anode contains Argon plasma, or negative glow. The Cathode has a Cathode glow, and the Anode has an Anode sheath. A Voltage vs. Distance graph shows the potential profile, with V_c at the cathode, 0 in the plasma, and V_p at the anode. A detailed view of the Al target shows Ar⁺ ions striking it, causing Al atoms to be ejected. These Al atoms travel through the negative glow and deposit on the Wafer surface.

- Most of voltage drop of the system (due to applied DC voltage, V_c) occurs over cathode sheath.
- Ar⁺ ions are accelerated across cathode sheath to the negatively charged cathode, striking that electrode (the “target”) and sputtering off atoms (e.g. Al). These travel through plasma and deposit on wafers sitting on anode.
- Rate of sputtering depends on the sputtering yield, Y , defined as the number of atoms or molecules ejected from the target per incident ion.
- Y is a function of the energy and mass of ions, and the target material. It is also a function of incident angle.

5/14/2012 ECE 416/516 Spring 2011 81

The diagrams illustrate flux arrival from a source to a wafer. Diagram a) shows isotropic flux arrival from a point source, where particles strike the wafer from all angles. Diagram b) shows anisotropic flux arrival from a large source, where particles strike the wafer from a wide range of angles. The mean free path λ is given by $mfp \lambda = kT / \sqrt{2\pi} d^2 P$, where $k = 1.36 \times 10^{-22} \text{ cc.atmos} / K$, $d = \text{collision } c/s \text{ in cm} \sim 4 \times 10^{-8} \text{ cm}$, and $P = \text{pressure (atmos)}$. For $P \sim 5 \text{ mtorr} \rightarrow mfp \lambda \sim 1 \text{ cm}$.

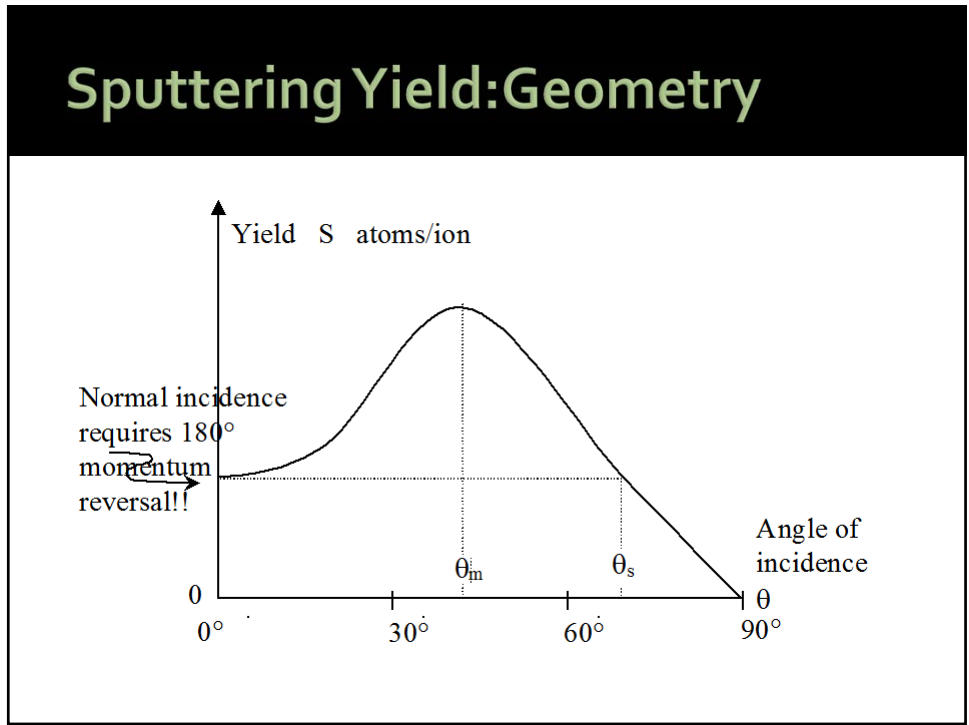
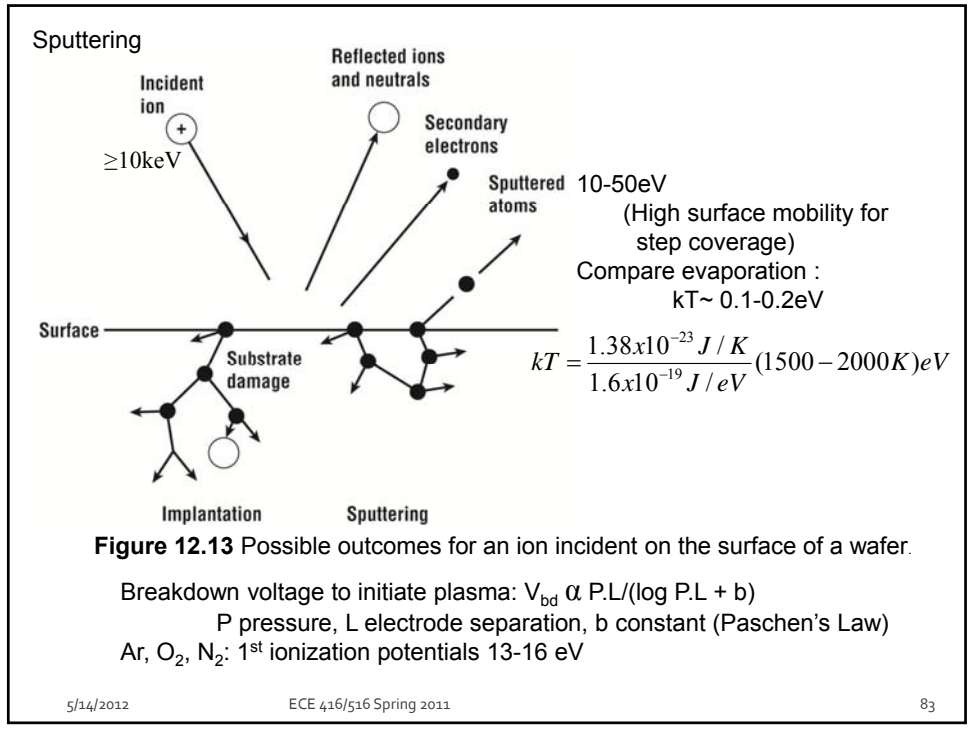
• Sputtering targets are generally large and provide a wide range of arrival angles in contrast to a point source.

a) Isotropic flux arrival $n = 1$ in $\cos^n \theta$ arrival angle distribution
 b) Anisotropic flux arrival $n > 1$ in $\cos^n \theta$ arrival angle distribution

The detailed view shows a small area at position i on the surface of the wafer. Flux F^0 is incident at an angle θ to the normal. The normal component of flux is $F^0 \cos \theta$.

- Arrival angle distribution generally described by a $\cos^n \theta$ distribution (the normal component of flux striking the surface determines the deposition or growth rate).
- Size and type of source, system geometry and collisions in gas phase important in arrival angle distribution.

5/14/2012 ECE 416/516 Spring 2011 82



Sputtering Yield: Energy

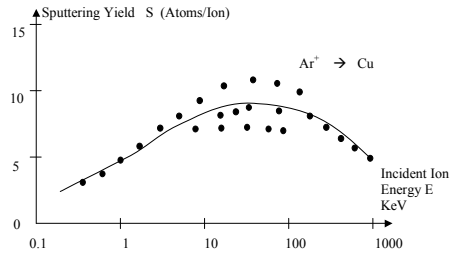
$$E < 1 \text{ keV} : S = 3\alpha/4\pi^2 * 4m_i m_t / (m_i + m_t)^2 * E/U_0$$

U_0 Surface binding energy of target

$$\alpha = f(m_t/m_i)$$

$$\mapsto 0.17, m_t = m_i/10$$

$$\mapsto 1.40, m_t = 10m_i$$

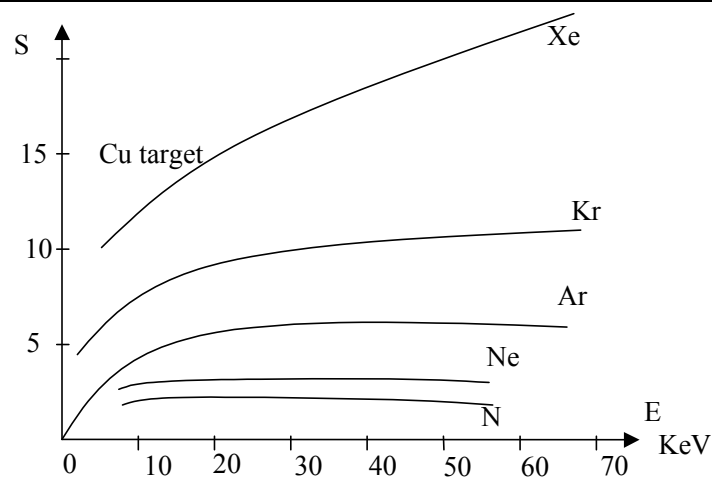


$E > 1 \text{ keV}:$

$$S = 3.56\alpha [Z_1 Z_t / (Z_1^{2/3} + Z_t^{2/3})] [m_i / (m_i + m_t)] S_n(E) / U_0$$

where $S_n(E)$ is reduced stopping power

Sputtering Yield: Gas



Sputtering Yield: Target

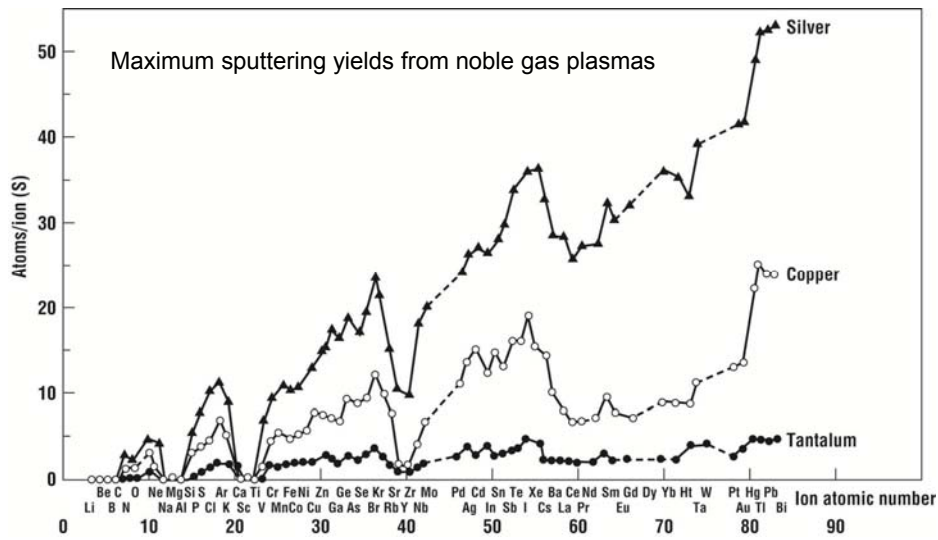
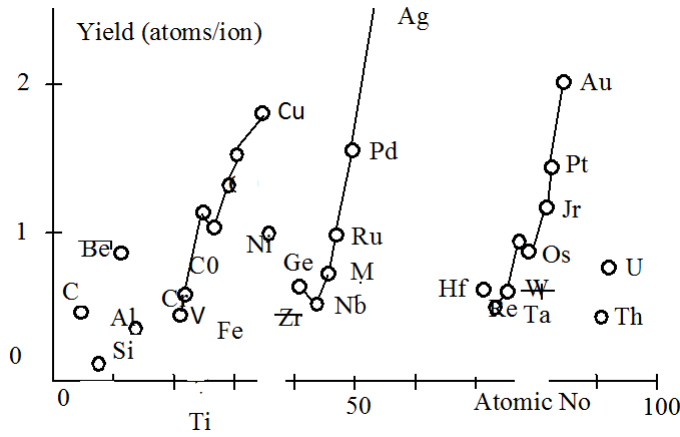
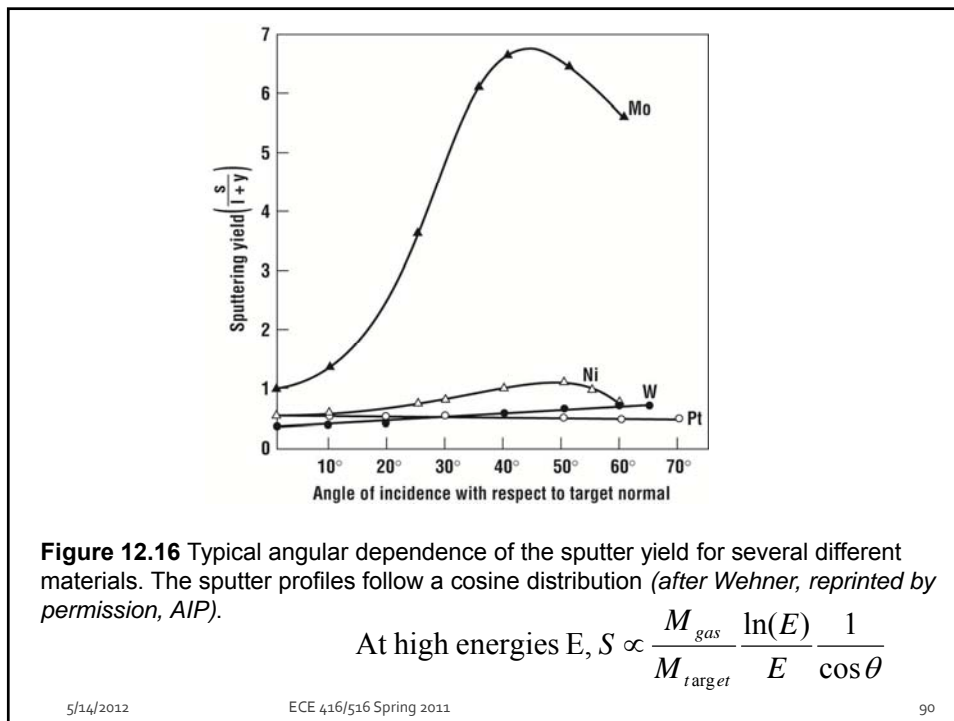
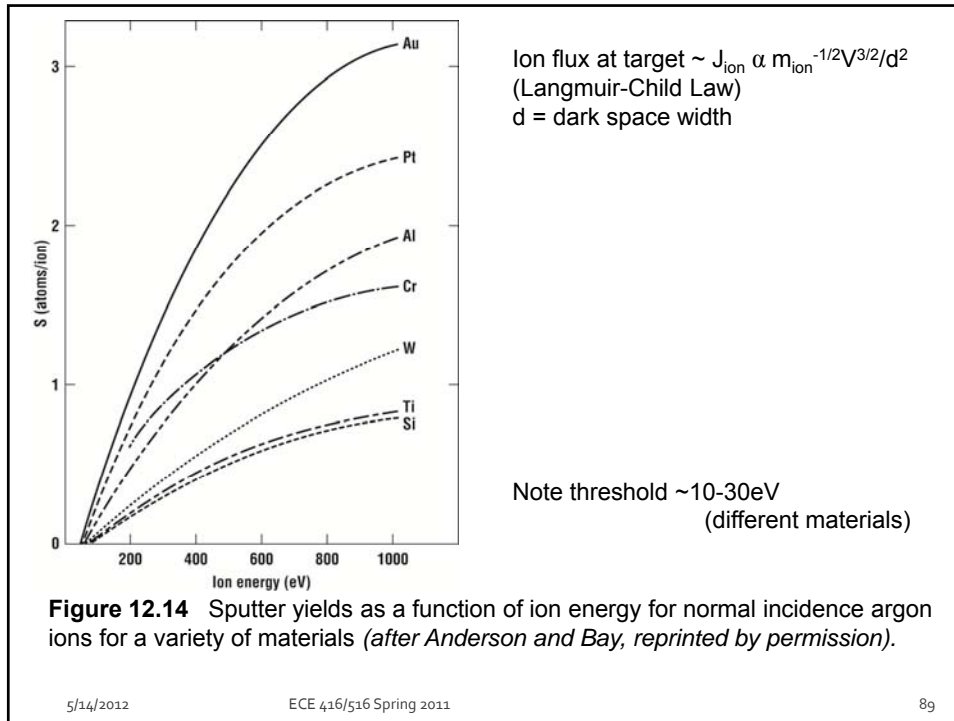
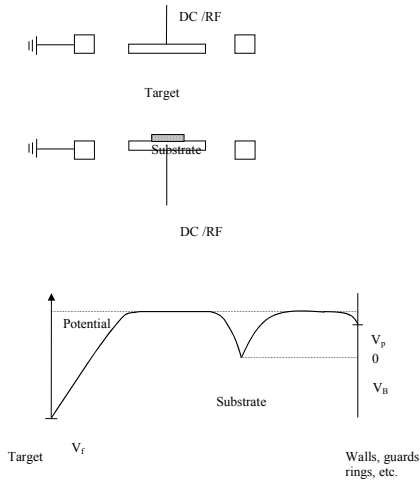


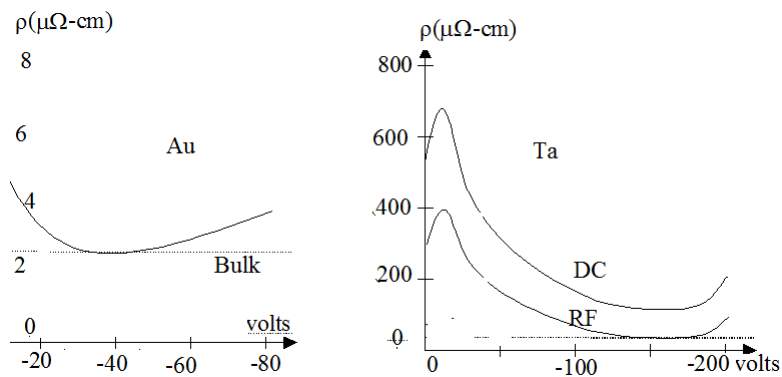
Figure 12.15 Sputter yield as a function of the bombarding ion atomic number for 45-keV ions incident on silver, copper, and tantalum targets (after Wehner, reprinted by permission, AIP).



Substrate Bias

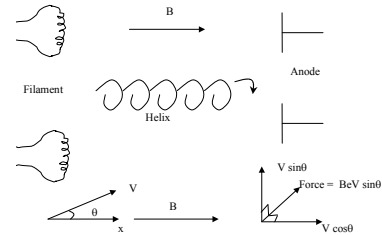


Effect of Substrate Bias



Magnetic Confinement

Uses axial field



$$m_e (V \sin \theta)^2 / r = Be V \sin \theta \rightarrow r = m_e V \sin \theta / Be$$

Negligible effect on ions

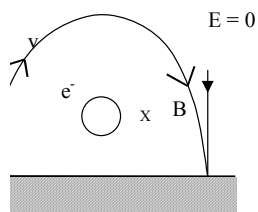
Confine electrons to minimize loss to walls, etc.

Results in increased ionization efficiency ($n_i = n_e$)

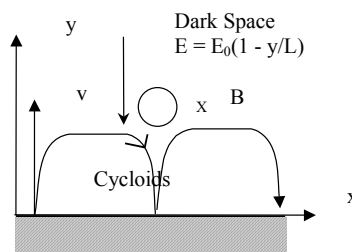
Increases ion current/sputtering rate

Can lead to non-uniform erosion

Magnetron



Secondary electrons returned to target

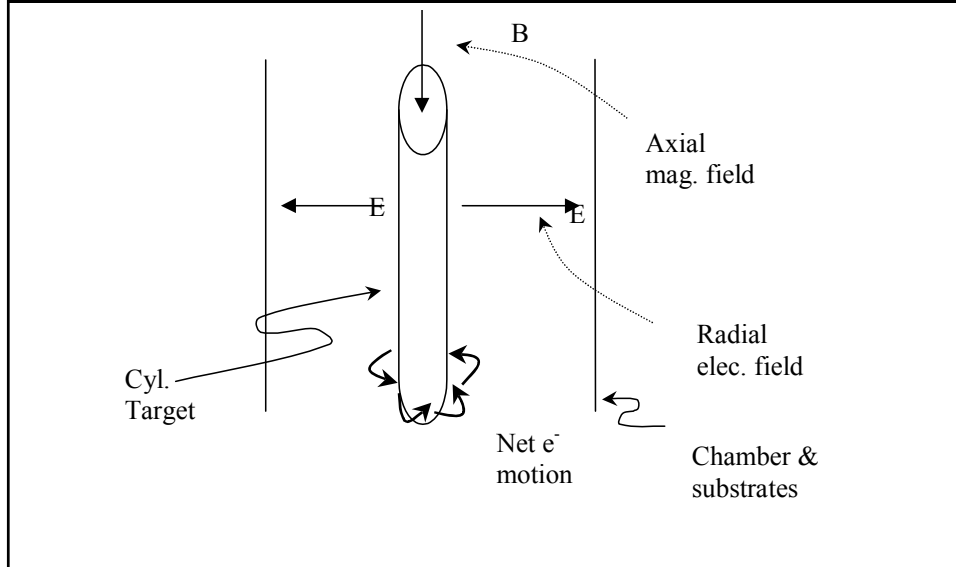


Max excursion from target

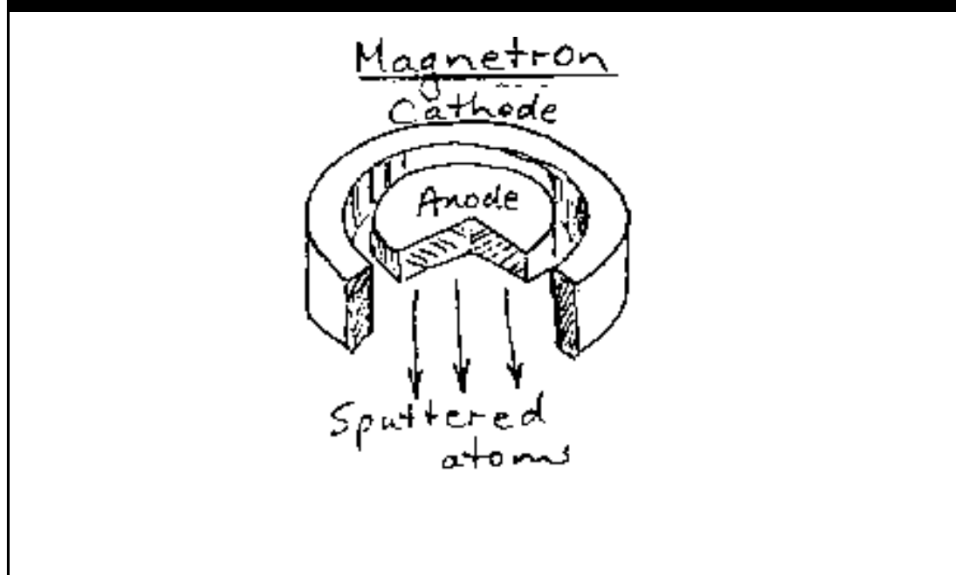
$$Y_{\max} = \sqrt{(2m/e)(v-v_T)/B}$$

at $Y_{\max} \uparrow \uparrow$ at target

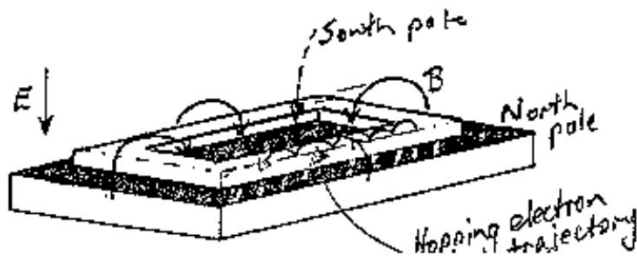
Cylindrical Magnetron



Circular Magnetron



Planar Magnetron



Magnetically confined plasma defines area of erosion

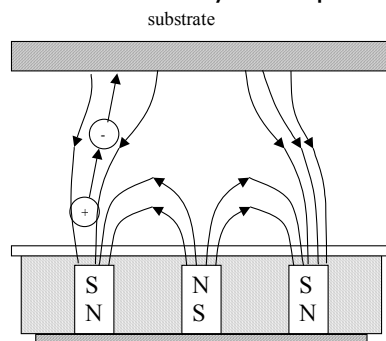
Unbalanced Magnetron

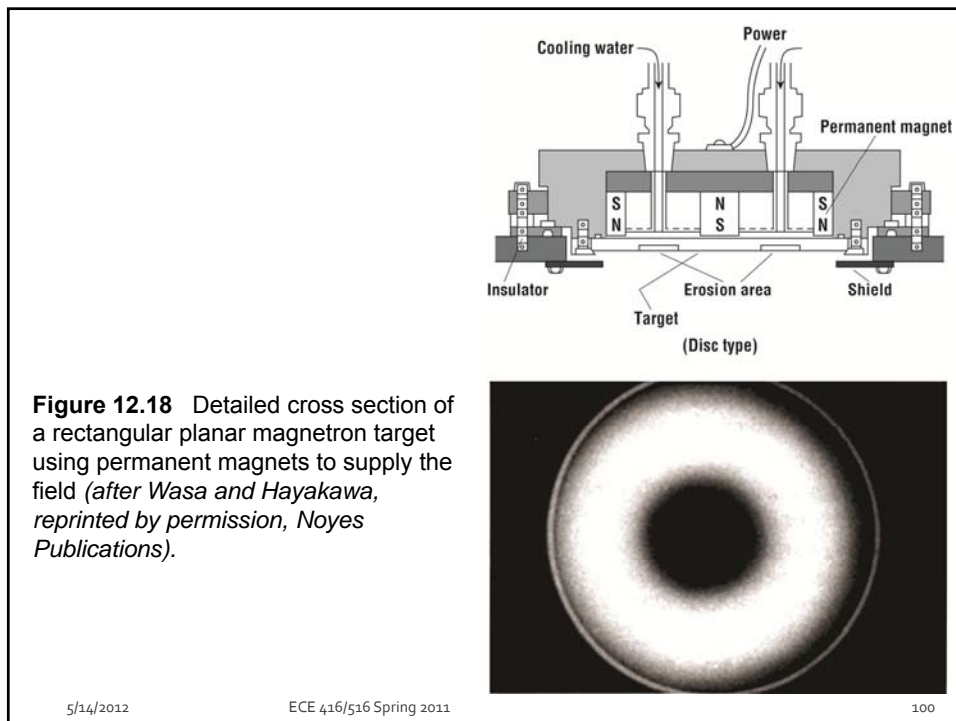
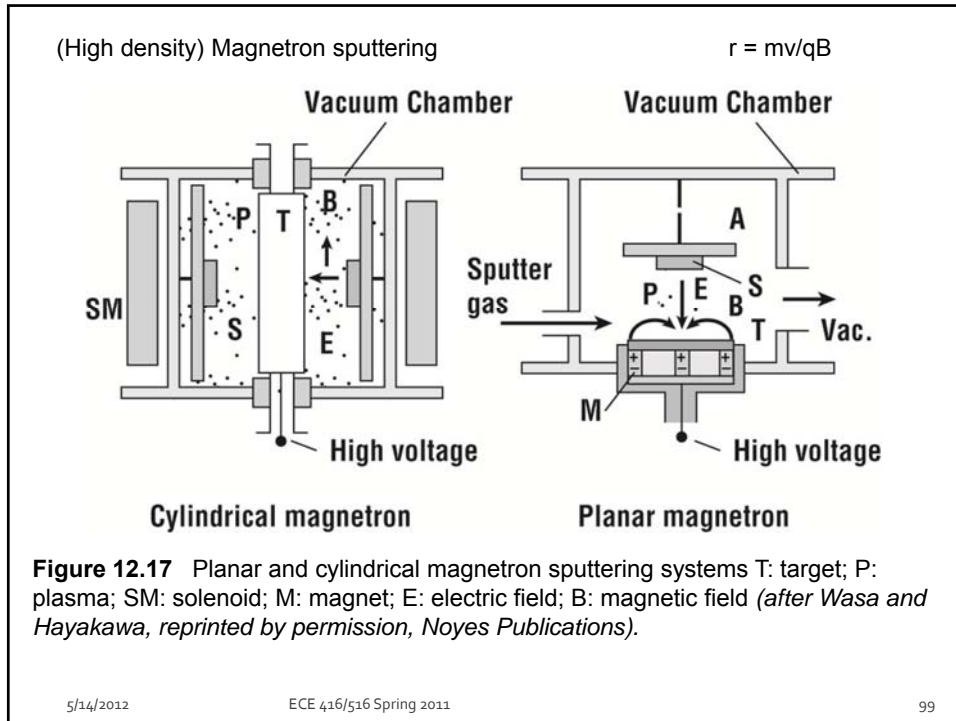
Central magnet weakened

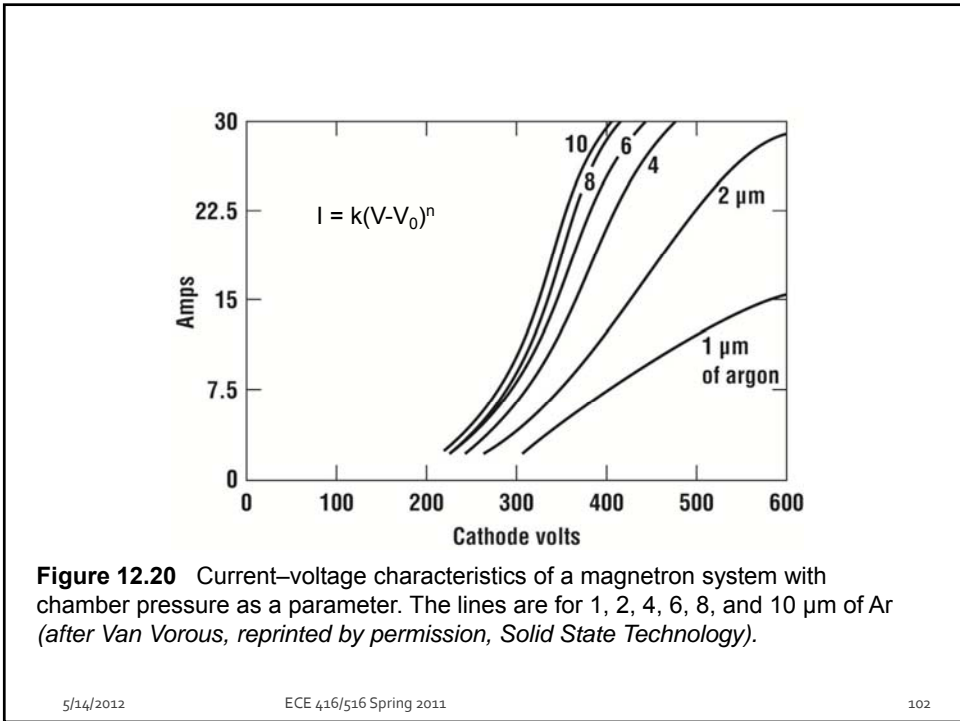
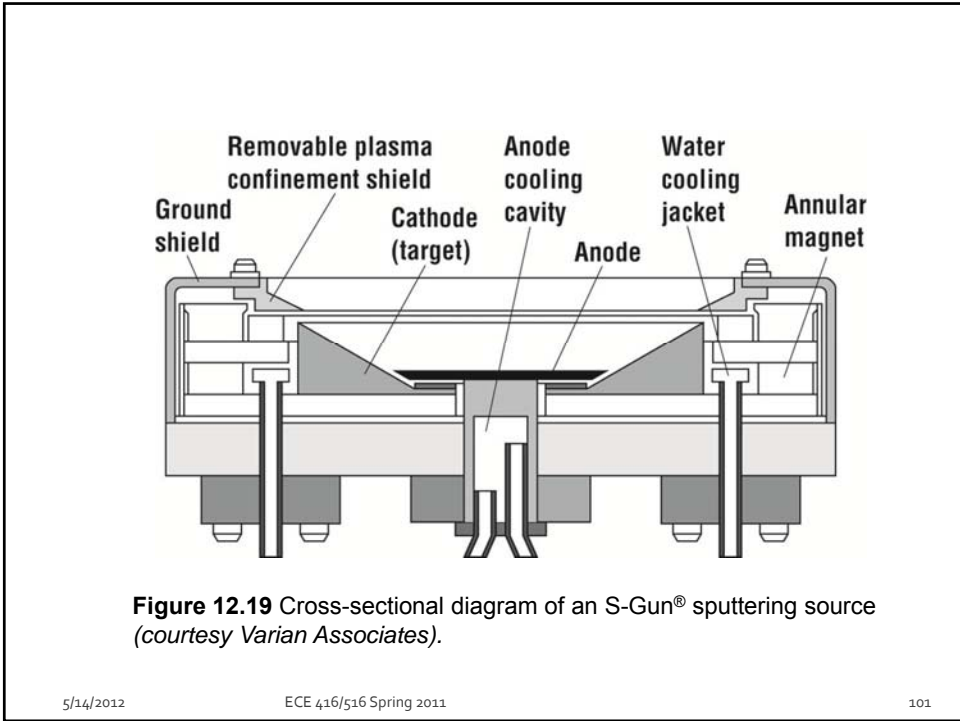
↳ field lines to substrate

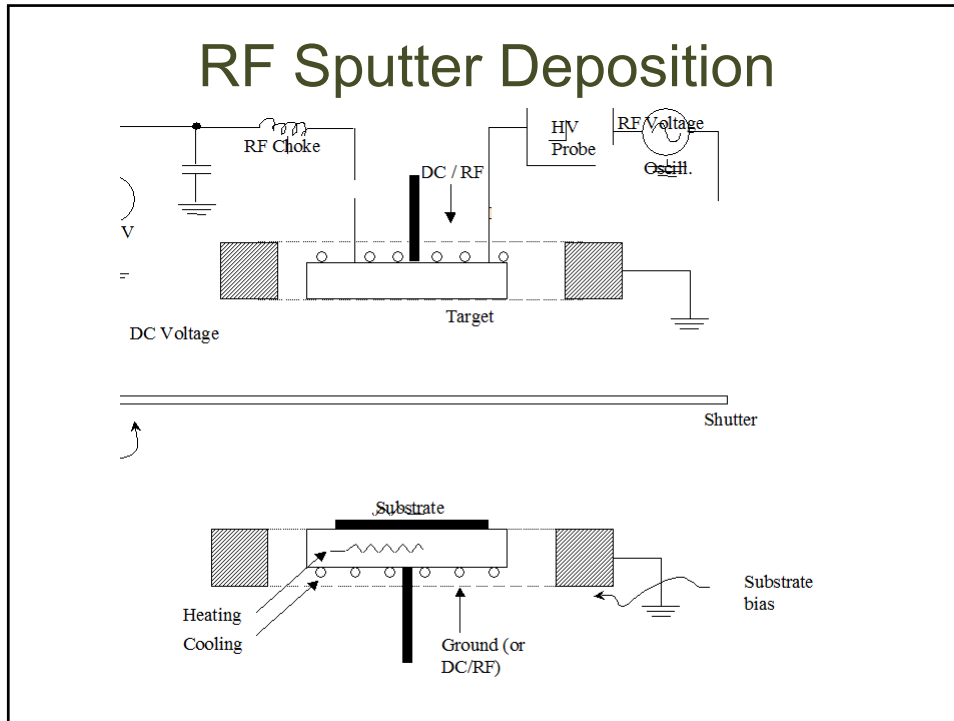
Electrons channeled to substrate

↳ ions by ambipolar diffusion









RF Sputter Deposition

The diagram shows the electrical setup for RF sputter deposition, including a matching network, RF generator, and the sputter chamber. The chamber contains an electrode/target, Argon plasma, wafers, electrode, and heater. A sputtering gas inlet (Ar) and vacuum outlet are also shown.

- For DC sputtering, target electrode is conducting.
- To sputter dielectric materials use RF power source.
- Due to slower mobility of ions vs. electrons, the plasma biases positively with respect to both electrodes. (DC current = zero.)
∴ continuous sputtering.
- When the electrode areas are not equal, the field must be higher at the smaller electrode (higher current density), to maintain overall current continuity

$$\frac{V_1}{V_2} = \left(\frac{A_2}{A_1}\right)^m \quad (m = 1-2 \text{ experimentally}) \quad (13)$$

- Thus by making the target electrode smaller, sputtering occurs "only" on the target. Wafer electrode can also be connected to chamber walls, further increasing V_2/V_1 .

The graph below shows the voltage distribution across the electrodes. For equal area electrodes, the voltage is uniform. For unequal area electrodes (smaller electrode at left), the voltage is higher at the smaller electrode, resulting in a higher current density.

Ionized Sputter Deposition or HDP Sputtering

DC target bias

Al target

Al →
Al⁺ + e⁻

Inductively coupled RF antenna

RF substrate bias

a) b)

- In some systems the depositing atoms themselves are ionized. An RF coil around the plasma induces collisions in the plasma creating the ions.
- This provides a narrow distribution of arrival angles which may be useful when filling or coating the bottom of deep contact hole.

5/14/2012 ECE 416/516 Spring 2011 105

Sputtering Contamination #1

Argon

Complexes ArH⁺, H₃O⁺, etc.

Contaminants

Photons

Negative ions

Fast & Slow electrons

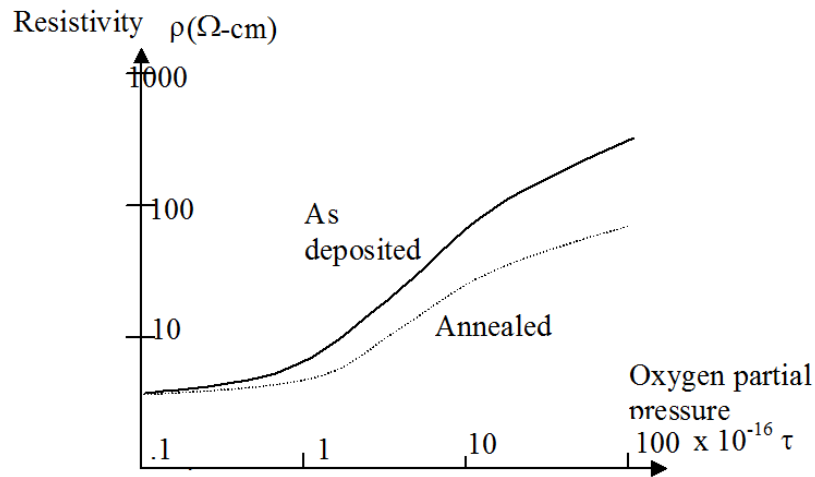
Sputtered Atoms

SUBSTRATE

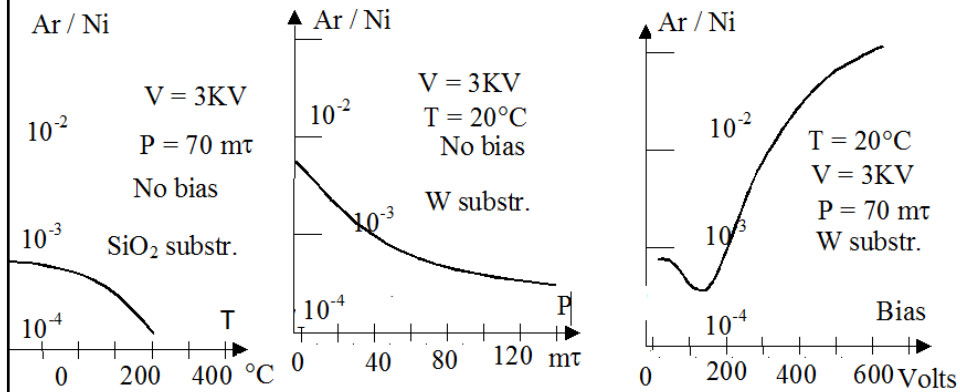
Argon: Thermal neutrals
Metastables
Ar²⁺ / Ar⁺ / Ar₂⁺
etc.

Fast (target)
Fast (charge-exchange)

Sputtering Contamination #2



Sputtering Contamination #3



Morphology

1. Low T, low E, high P → amorphous
 T: Decr P, incr T → small grains (often optimum for thin film purpose)
2. Incr T &/or E → grain incr (tall narrow grains)
3. Incr T &/or E → large 3D grains (single crystal, epitaxy?)
 Note: 2 & 3 → rough surfaces

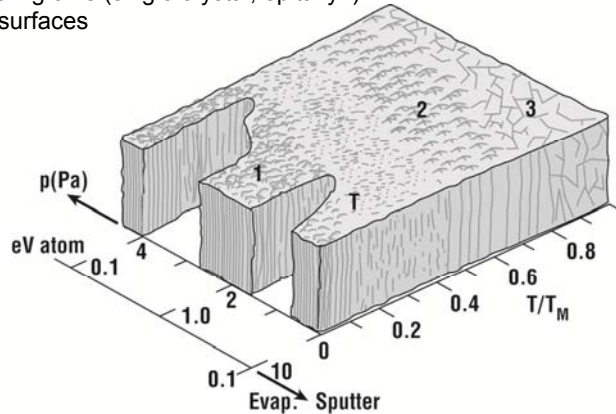


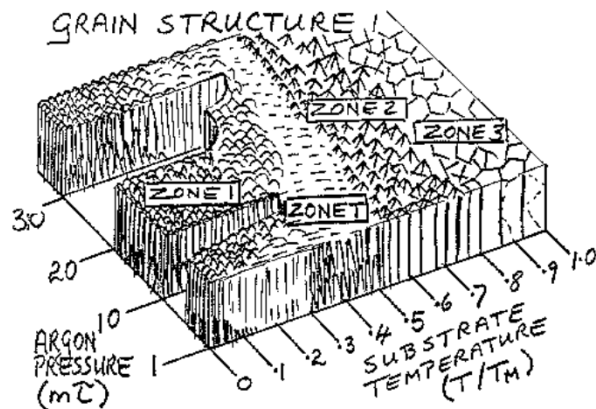
Figure 12.21 The three-zone model of film deposition as proposed by Movchan and Demchishin (after Thornton, reprinted by permission, AIP).

5/14/2012

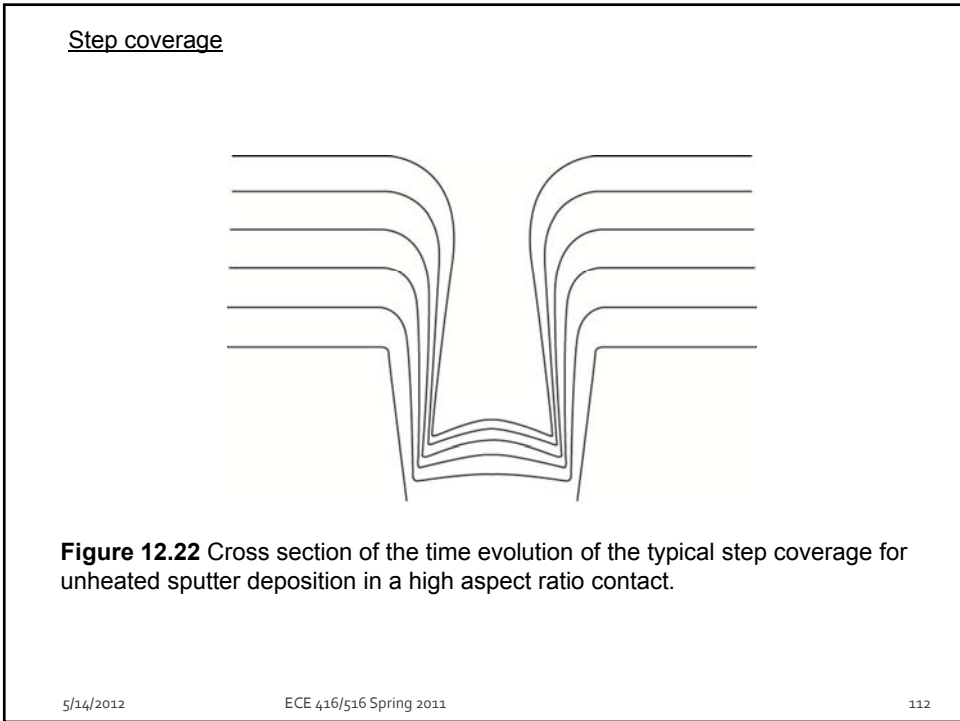
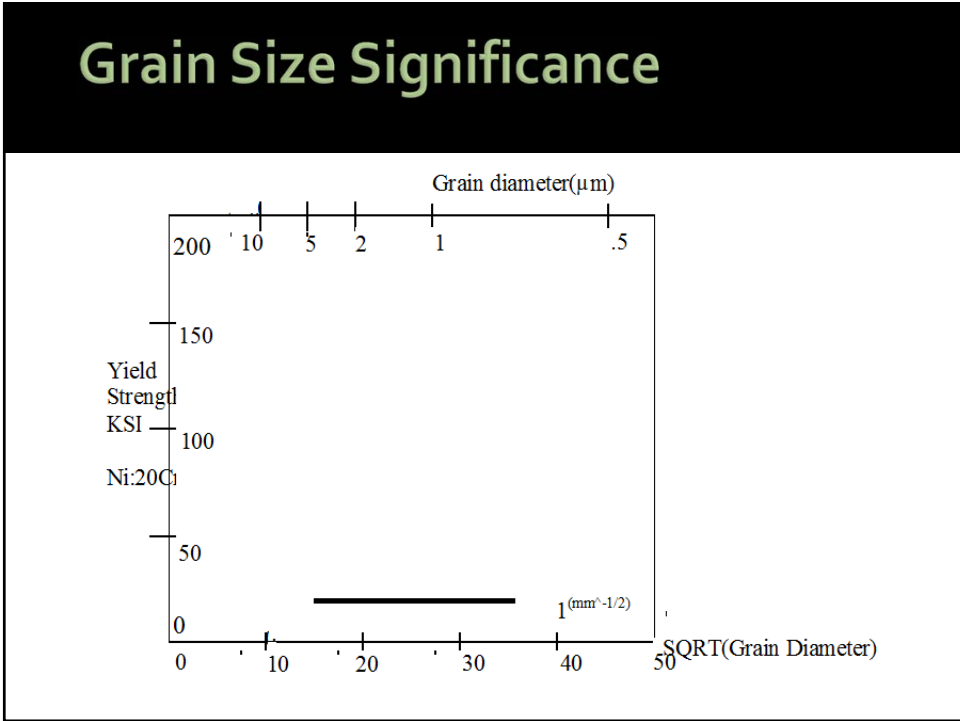
ECE 416/516 Spring 2011

109

Grain Structure



- Zone 1: Porous structure, tapered crystallites sep'd by voids
- Zone 2: Columnar grains; Zone 3: Recrystallized grain structure
- Zone T: Transition structure:-Densely packed fibrous grains



Models and Simulation

- Within the past decade, a number of simulation tools have been developed for topography simulation.
- Generalized picture of fluxes involved in deposition. (No gas phase boundary layer is included, so this picture doesn't fully model APCVD.)
- Essentially the same picture can be used for etching simulation

$$F_{net}^i = F_{direct(neutrals)}^i + F_{direct(ions)}^i + F_{redep}^i + F_{diff.in}^i - F_{emitted}^i - F_{sputtered}^i - F_{diff.out}^i \quad (14)$$

- To simulate these processes, we need mathematical descriptions of the various fluxes.
- Modeling specific systems involves figuring out which of these fluxes needs to be included.

5/14/2012 ECE 416/516 Spring 2011 113

- Direct fluxes ($F_{direct(neutrals)}^i + F_{direct(ions)}^i$) are generally modeled with an arrival angle distribution just above the wafer (doesn't model equipment).

$$F_{direct}(\theta) = F^0 \cos^n \theta \quad (15)$$

- $F_{direct}(\theta)$ is the normal component of the incoming flux (which is what is needed in determining the growth rate).
- Higher pressure systems \Rightarrow more gas phase collisions, shorter mean free path $\Rightarrow n = 1$ (isotropic arrival).
- Lower pressure systems \Rightarrow fewer gas phase collisions, longer mean free path $\Rightarrow n > 1$ (anisotropic arrival).
- Ionic species in biased systems \Rightarrow directed arrival $\Rightarrow n > 1$ (anisotropic arrival).
- Once the direct fluxes are known, surface topography must be considered.
- Surface orientation, viewing angle and shadowing are important. Gas phase collisions are neglected near the wafer surface.

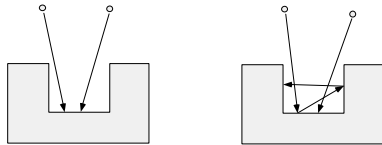
5/14/2012 ECE 416/516 Spring 2011 114

- The indirect fluxes are associated with processes on the wafer surface.
- Surface diffusion is driven by the local curvature of the surface (to minimize the surface free energy) and is given by

$$F_{diff.in} - F_{diff.out} = F_{diff.net} = \frac{D_s}{kT} \gamma_s \Omega v \frac{\partial^2 K}{\partial s^2} \quad (16)$$

where D_s is the surface diffusivity, γ_s is the surface energy, K is the curvature and Ω and v are constants.

- Surface diffusion helps to fill in holes, and produces more planar depositions because molecules can diffuse to "smooth out" the topography.



High ($S_c = 1$)

Low ($S_c < 1$)

- $F_{emitted}^i$ arises because not all molecules "stick" when they arrive at the surface.

$$F_{emitted}^i = (1 - S_c) F_{incident}^i \quad (17)$$

where S_c is the sticking coefficient.

$$S_c = \frac{F_{reacted}}{F_{incident}} \quad (18)$$

- Generally ions are assumed to stick ($S_c = 1$), neutrals have $S_c < 1$ and are assumed to be emitted with a $\cos \theta$ angle distribution (no memory of arrival angle).

5/14/2012

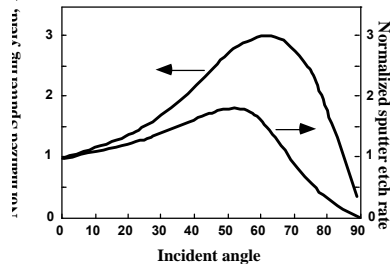
ECE 416/516 Spring 2011

115

- $F_{redep(emitted)}^i$ arises because the emitted flux $F_{emitted}^i$ can land elsewhere on the surface. Thus

$$F_{redep(emitted)}^{ik} = g^{ik} * F_{emitted}^k = g^{ik} * (1 - S_c) * F^k \quad (19)$$

- The redeposited flux at point i due to an emitted flux at point k . g^{ik} accounts for the geometry between i and k .
- Thus a low $S_c < 1$ can produce more conformal coverage because of emission/redeposition (usually more important than surface diffusion in CVD).



- The sputtered flux is caused primarily by energetic incoming ions.

$$F_{sputtered}^i = Y * (F_{argon}^i + F_{direct(ions)}^i) = Y * F_{ions}^i \quad (20)$$

- where Y is the sputtering yield.
- Y is angle sensitive which can be used to achieve more planar surfaces during deposition (example later).

- The sputtered molecules can be redeposited. This is modeled as in Eqn. (19), i.e.

$$F_{redep(sput)}^{ik} = g^{ik} * F_{sputtered}^k = g^{ik} * Y * F_{ions}^k \quad (21)$$

5/14/2012

ECE 416/516 Spring 2011

116

PVD Deposition Systems

- Standard PVD systems might include DC and RF sputtering systems and evaporation systems.
- Ions generally do not play a significant role in these systems, so modeling is similar to LPCVD systems.

Thus $\text{rate} = \frac{S_c F_d}{N}$ (26)

- The values for S_c and F_d would be different for LPCVD and PVD systems however.
- Sometimes these systems are operated at high temperatures, so a surface diffusion term must be added.

$$\text{rate} = \frac{S_c F_d + \frac{D_s}{kT} \gamma_s \Omega v \frac{\partial^2 K}{\partial s^2}}{N}$$
 (27)

5/14/2012 ECE 416/516 Spring 2011 117

Ionized PVD Deposition Systems

- These systems are complex to model because both ions and neutrals play a role.
- They are often used for metal deposition so that Ar^+ ions in addition to Al^+ or Ti^+ ions may be present.
- Thus almost all the possible terms are included

F_{direct}^i (neutrals)	Yes
F_{direct}^i (ions)	Yes
F_{diff}^i (net) = F_{diff}^i (in) - F_{diff}^i (out)	No
F_{emitted}^i	Yes
F_{redep}^i (emitted)	Yes
$F_{\text{sputtered}}^i$	Yes
F_{redep}^i (sputtered)	Yes
$F_{\text{ion-induced}}^i$	Yes

$$\text{rate} = \frac{(S_c F_d) + F_i - (K_{sp} Y F_i) + (K_{rd} F_{rd})}{N}$$

where F_d includes the direct and redeeposited (emitted) neutral fluxes, F_i includes the direct and ion-induced fluxes associated with the ions, and F_{rd} models redeposition due to sputtering.

5/14/2012 ECE 416/516 Spring 2011 118

Wafer heating

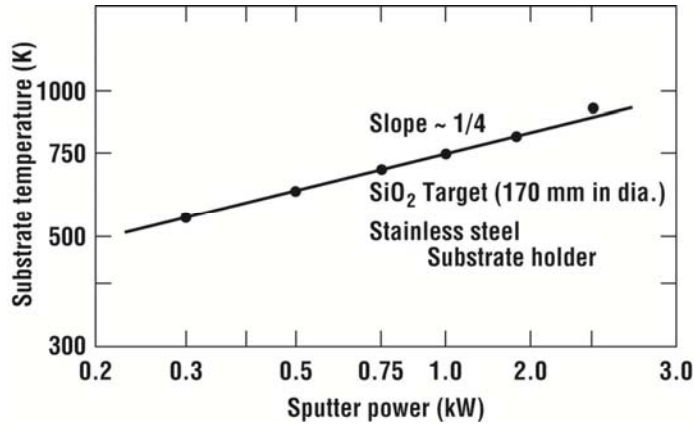


Figure 12.23 The temperature rise of substrates as a function of the plasma power for an argon RF plasma with an SiO₂ target (after Wasa and Hayakawa, reprinted by permission, Noyes Publications).

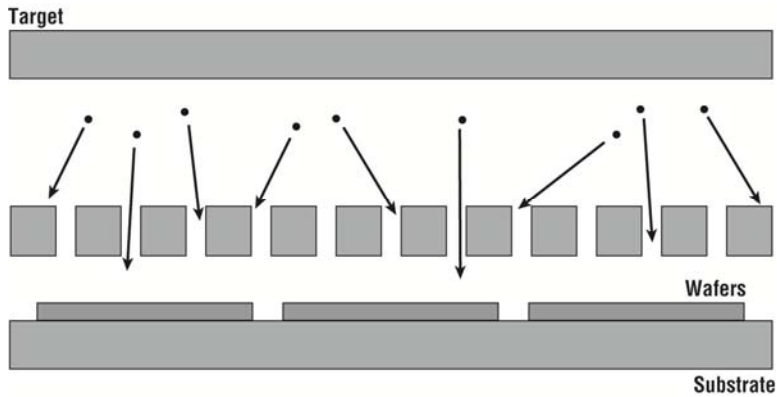


Figure 12.24 In collimated sputtering a disposable collimator is placed close to the wafers to increase directionality.

Ions ~ perpendicular to surface



Figure 12.25 The Endura system by Applied Materials uses a number of PVD or CVD chambers fed by a central robot. For conventional and IMP (ionized metal plasma) sputtering, targets are hinged to open upward. Two open chambers are shown, along with the load lock (from Applied Materials).

5/14/2012

ECE 416/516 Spring 2011

121

(Negative) Bias sputtering

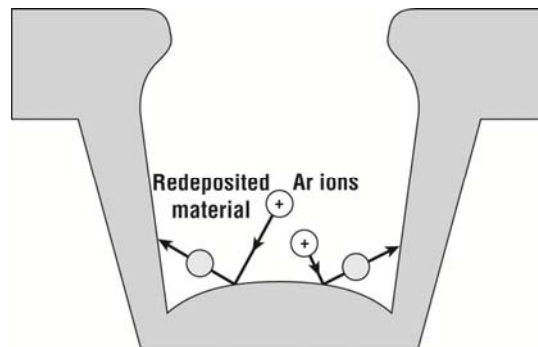


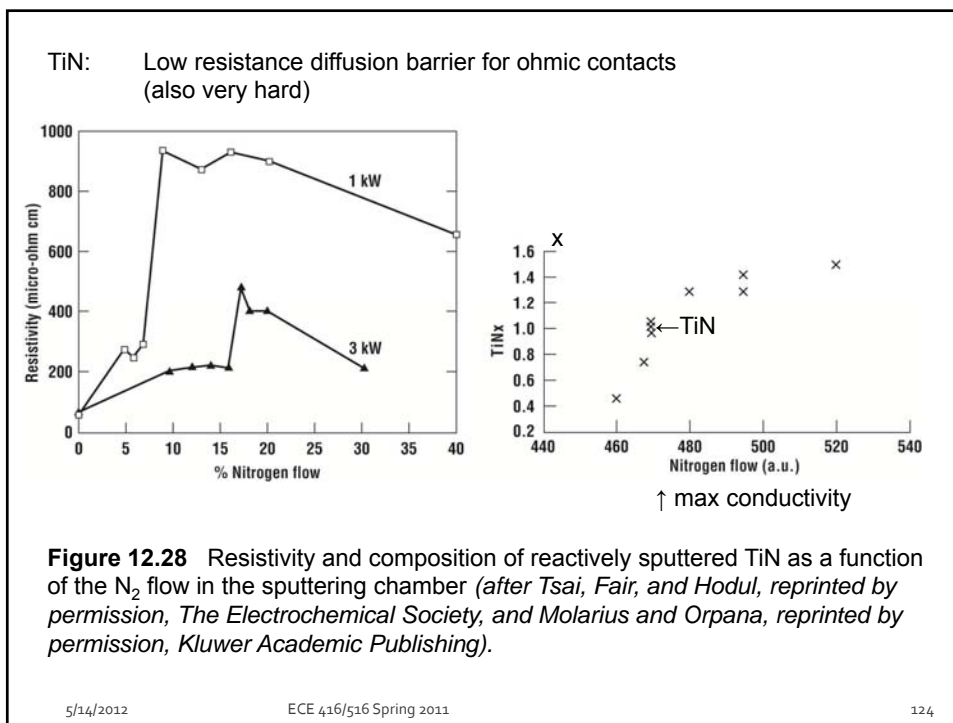
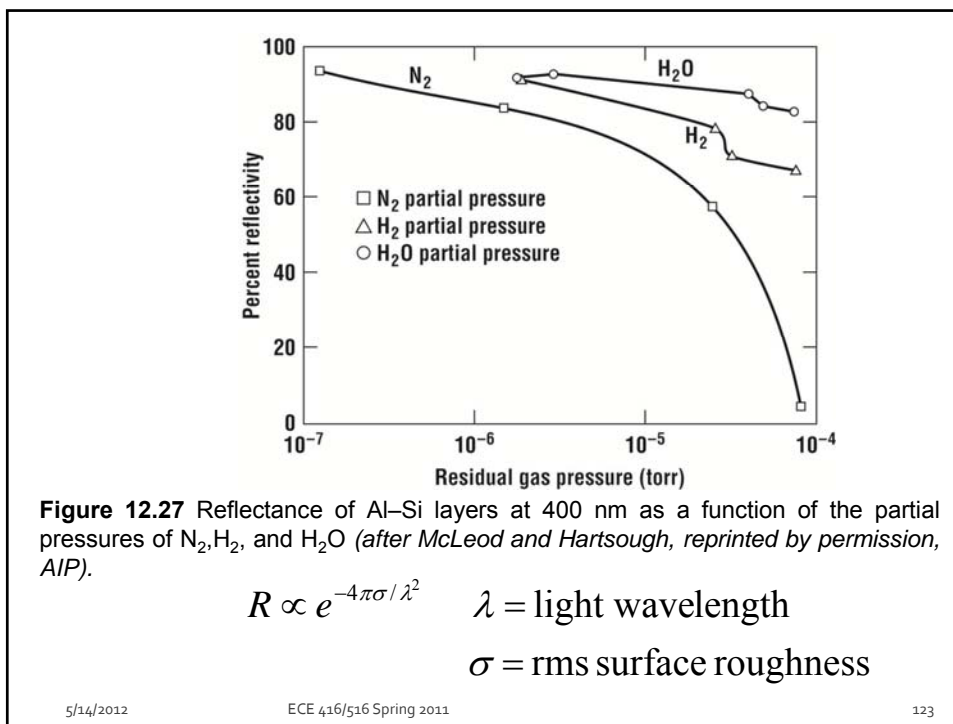
Figure 12.26 In bias sputtering, the ions incident on the surface of the wafer redistribute the deposited film to improve step coverage.

Ion Plating

5/14/2012

ECE 416/516 Spring 2011

122



High aspect ratio step coverage

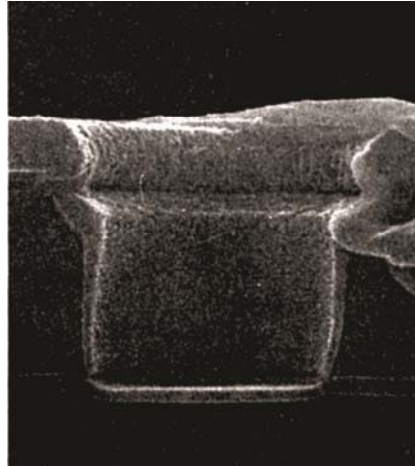


Figure 12.29 Cross section electron micrograph of a moderately high aspect ratio contact that has been sputter-deposited with TiN (after Kohlhase, Mändl, and Pamler, reprinted by permission, AIP).

5/14/2012

ECE 416/516 Spring 2011

125

Thin film stress

Thermal stress (thermomechanical stress) due to deposition at $T > T_{amb}$

$$\sigma_{th} = \frac{E_{film}}{1 - \nu_{film}} \int_{T_0}^{T_{dep}} (\alpha_{film} - \alpha_{sub}) dT, \text{ where } E = \text{Young's modulus, } \nu = \text{Poisson's ratio}$$

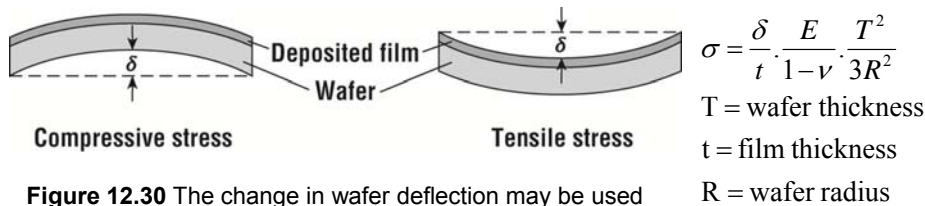


Figure 12.30 The change in wafer deflection may be used to measure the stress in a deposited layer. This is typically measured using a reflected laser beam.

$$\sigma = \sigma_{th} + \sigma_i$$

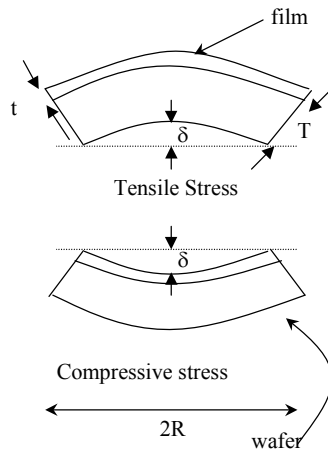
Intrinsic stress: Grain growth after deposition
Also, stress due to incorporated impurities (Ar)

5/14/2012

ECE 416/516 Spring 2011

126

Thin Film Stress #1

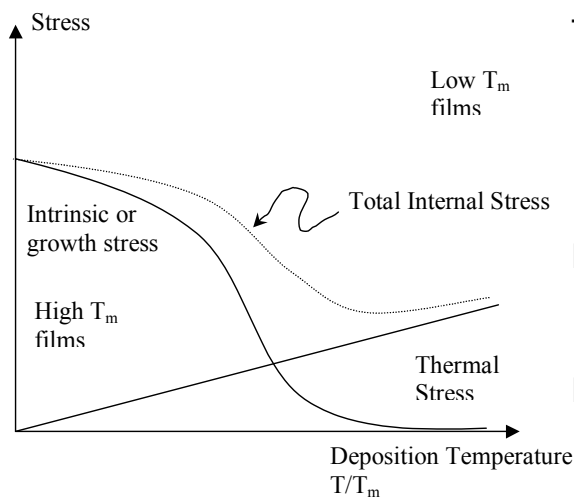


Stress $\sigma = (\delta/t)(T^2/3R^2) E_f/(1-\nu_f)$
 E_f = Young's modulus for film
 ν_f = Poisson's ratio for film

$$\sigma = \sigma_{\text{thermal}} + \sigma_{\text{intrinsic}}$$

$$\sigma_{\text{thermal}} = [E_f/(1-\nu_f)] \int_{T_0}^{T_{\text{dep}}} (\alpha_{\text{film}} - \alpha_{\text{sub}}) dT$$

Internal Stress

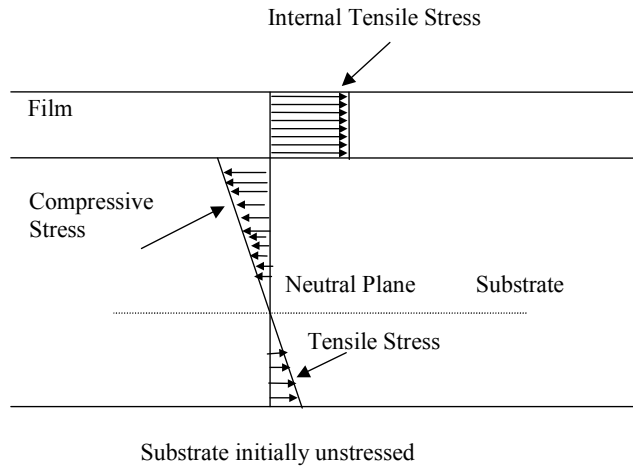


Thermal Stress:- mismatch of thermal coefficients of expansion of substrate & film.

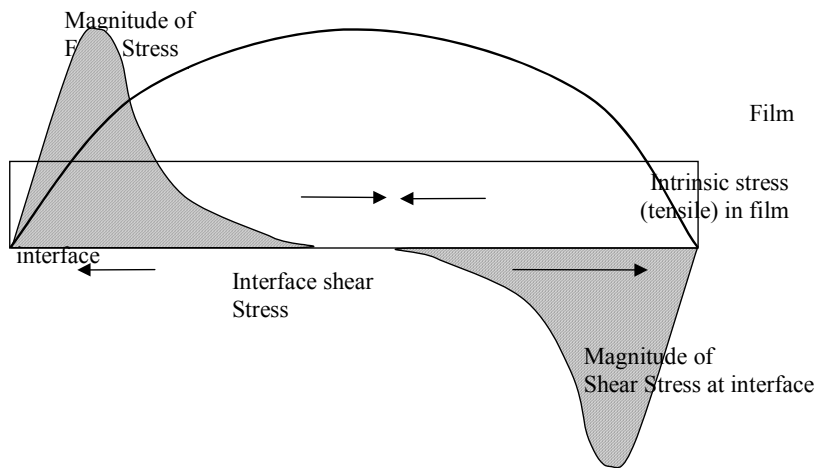
Intrinsic Stress:- due to growth of film, distortion of lattice.

Determine by measuring total stress & subtract thermal.

Stress Distribution

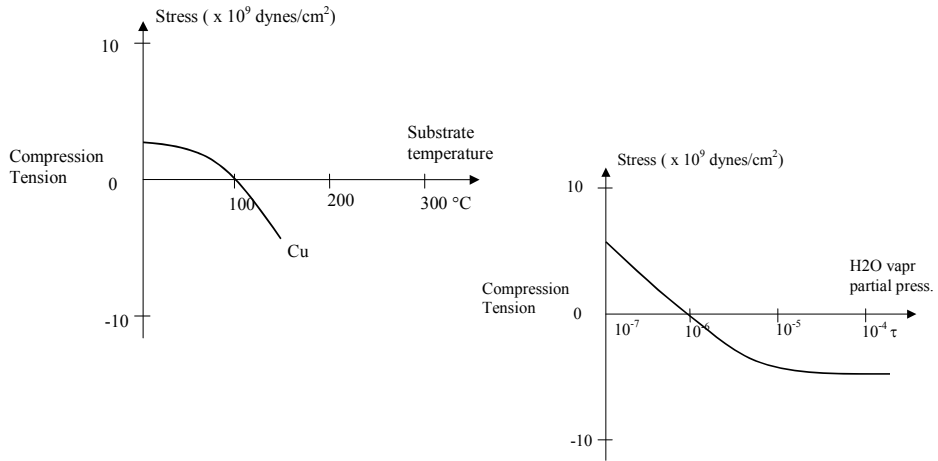


Interface Shear Forces



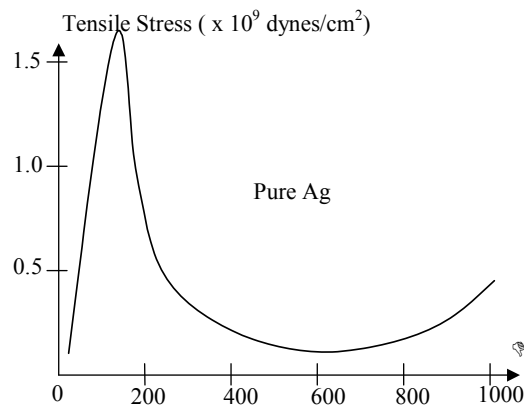
Stress: Evaporated Films #1

After removal of thermal stress effects



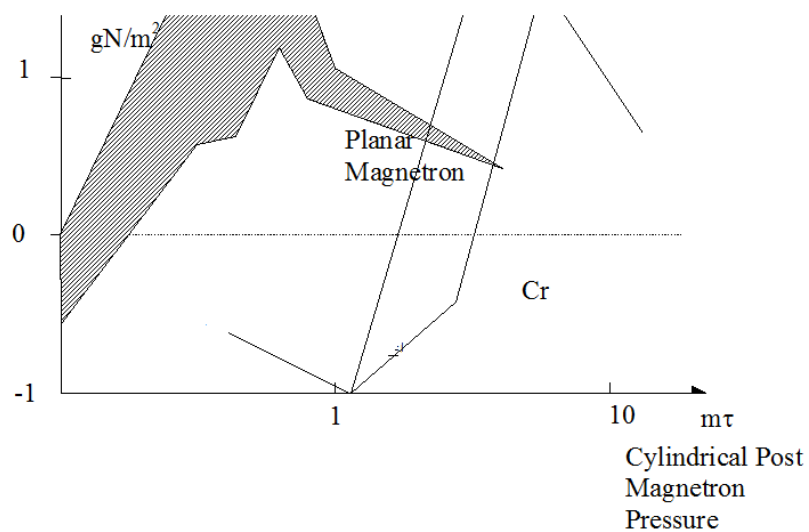
Compressive stress commonly due to contaminants

Stress: Evaporated Films

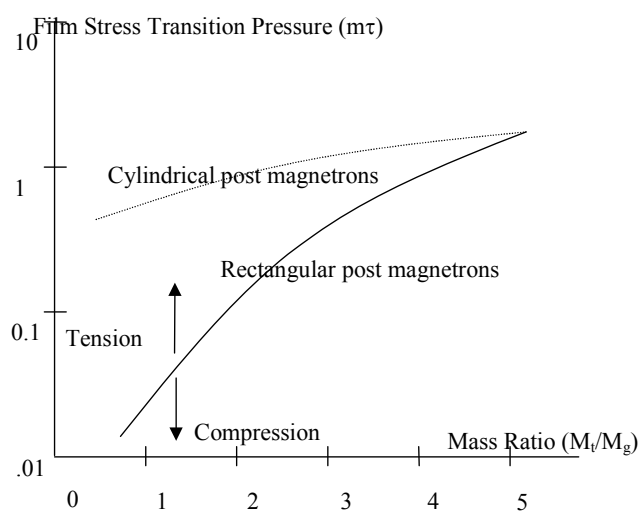


Max stress as last voids fill as film becomes fully continuous.

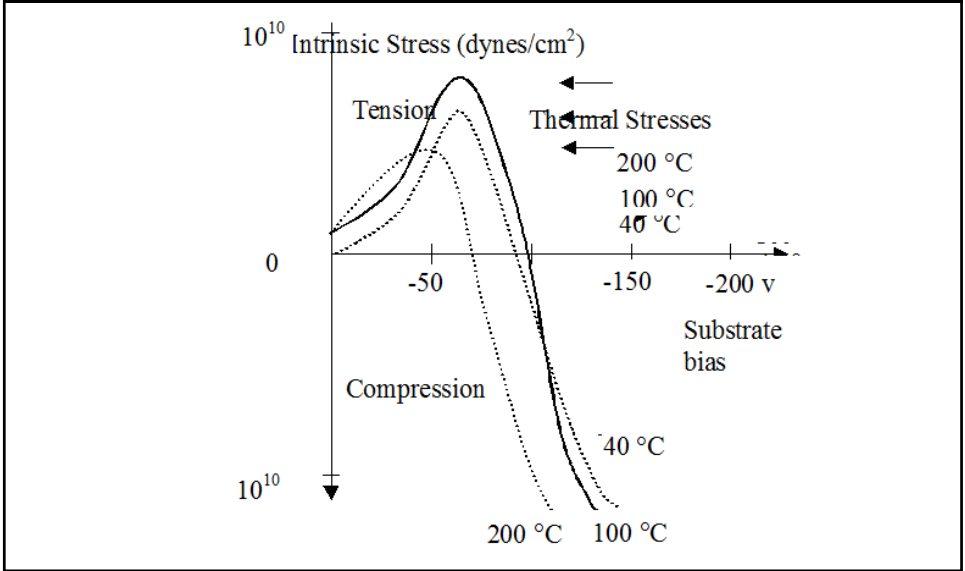
Stress:Sputtered Films #1



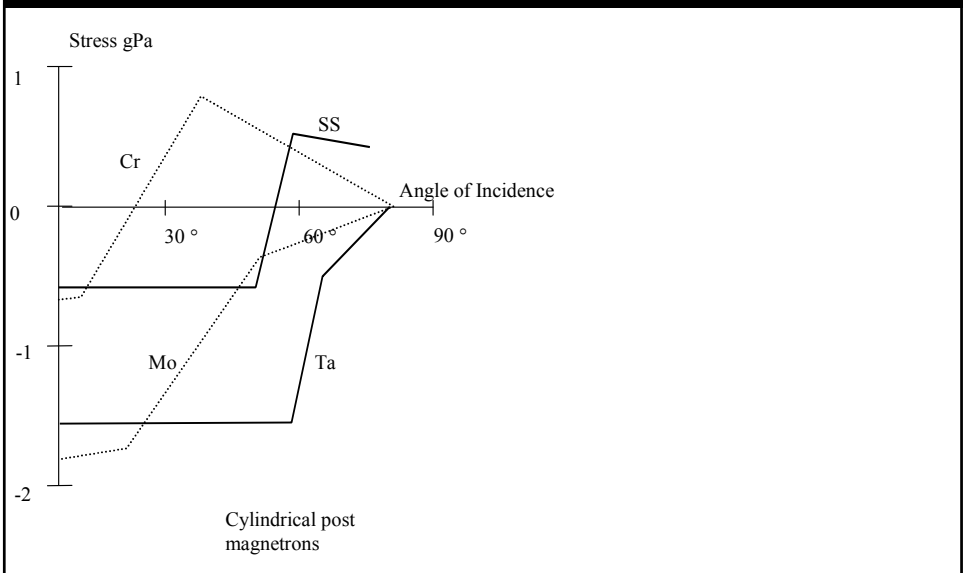
Stress:Sputtered Films #2



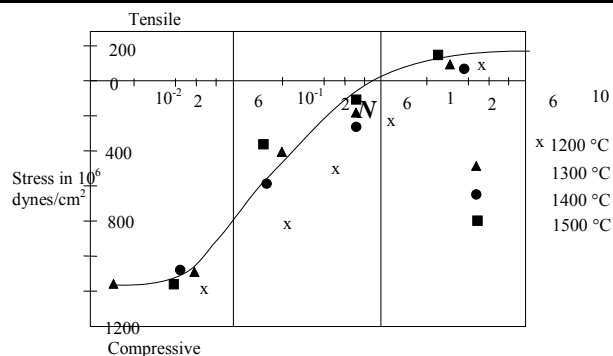
Stress:Sputtered Films #3



Stress:Sputtered Films #4

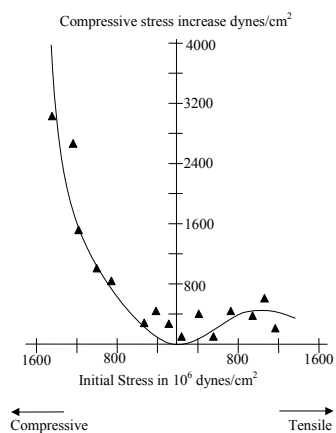


Stress:Sputtered Films #5

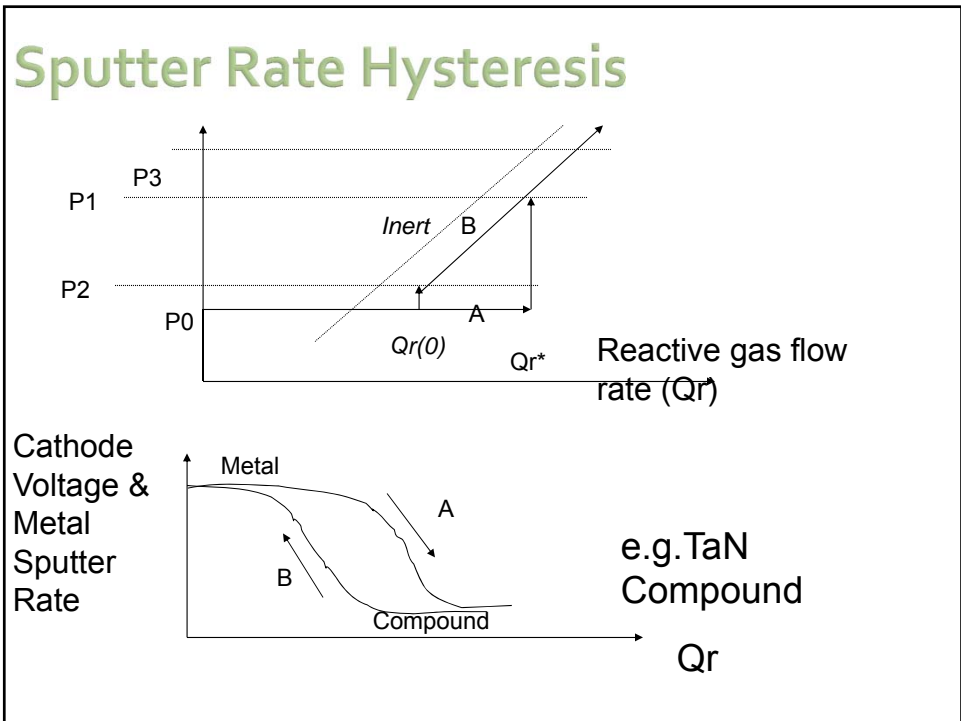
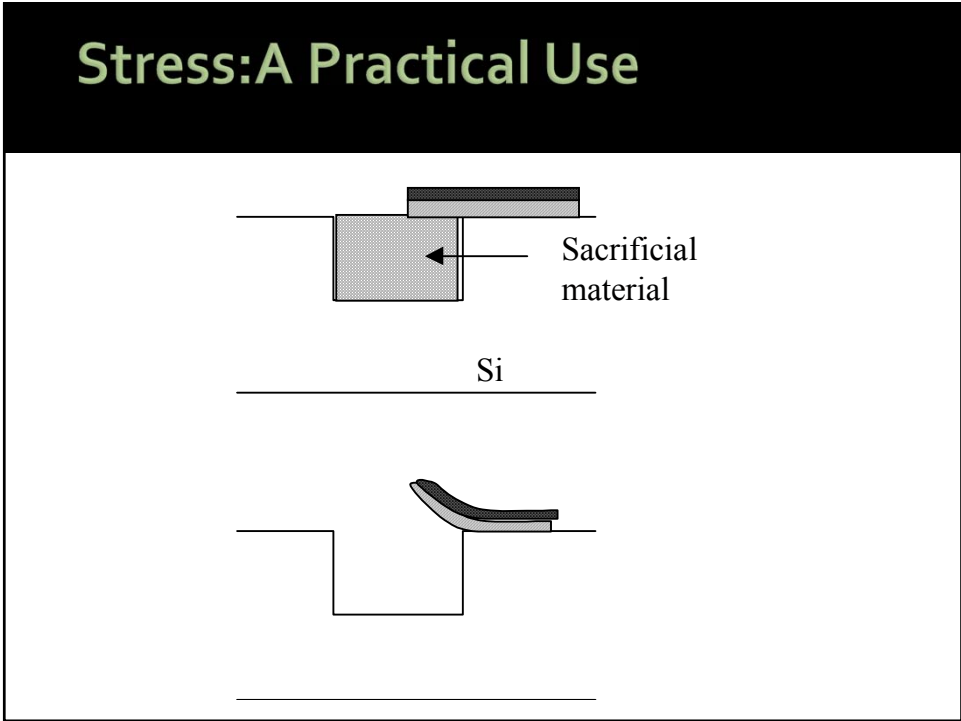


Stress of Silicon oxide films deposited in residual O₂ as a function of log N. (N = number of silicon monoxide molecules/number of residual gas molecules impinging on the substrate per unit area and time.)

Stress:Sputtered Films #6



Increase in compressive stress observed on evaporated SiO films after exposure to air



Summary of Key Ideas

- Thin film deposition is a key technology in modern IC fabrication.
- Topography coverage issues and filling issues are very important, especially as geometries continue to decrease.
- CVD and PVD are the two principal deposition techniques.
- In PVD systems arrival angle distribution is very important in determining surface coverage. Shadowing can be very important.
- A wide variety of systems are used in manufacturing for depositing specific thin films, e.g. magnetron sputtering.
- Advanced simulation tools are becoming available, which are very useful in predicting topographic issues.
- Generally these simulators are based on physical models of mass transport and surface reactions and utilize parameters like arrival angle and sticking coefficients from direct and indirect fluxes to model local deposition rates.
- Thin film stress can be due to differential CTEs, impurities, and grain growth.

5/14/2012

ECE 416/516 Spring 2011

141

Summary

- Various evaporation sources
- Evaporation rate from vapor pressure
- Deposition geometrics
- Alloy composition and contamination
- Rate & thickness monitors
- Nucleation theory
 - Capillary model
 - ⇒ critical nucleus
 - ⇒ nucleation rate
- Physics of sputtering
- RF and Magnetron Sputtering
- Film Contamination
- Film Stress
- (Thornton diagram)

Assignment #6

- 11.2
- 11.5

- 12.1
- 12.3
- 12.6
- 12.10